I&EC research
Industrial & Engineering Chemistry Research

pubs.acs.org/IECR

Article

Wall Slip and Flow Characteristics of Gas−Liquid−Solid Phase Coupling Flowing in Horizontal Pipelines

Lintong Hou, Dong Zhang, Meng Yang, Shuo Liu, and Jingyu Xu*

Cite This: *Ind. Eng. Chem. Res.* 2022, 61, 4951−4970

Read Online

ACCESS | Metrics & More | Article Recommendations

ABSTRACT: To investigate the multiphase coupled flow characteristics and apparent wall slip phenomenon in horizontal pipes, air−hydraulic oil−solid mixtures flowing in 50 mm-diameter and 32 mm-diameter pipes are tested. The results show that the critical liquid velocity corresponding to the transformation of the flow structure is between 0.75 and 1 m/s. Compared to the liquid−solid flow, the injection of gas has a drag reduction effect, to a certain extent. However, with an increase in the superficial gas velocity, the relative slip contribution first increased and then decreased. Moreover, the pressure gradient and wall slip velocity of the gas−liquid−solid coupling flow were sensitive to the superficial velocity of the gas and liquid phase and the phase volume fraction, as well as pipe conditions, including the diameter and roughness. Finally, on the basis of theoretical and experimental data, a wall slip model is proposed to predict the apparent wall slip velocity and pressure gradient in gas−liquid−solid coupled flow. The model shows that the apparent wall slip effect is promoted under the condition of a low volume fraction of the dispersed phase. Compared with the experimental data, the prediction results of the model are acceptable.

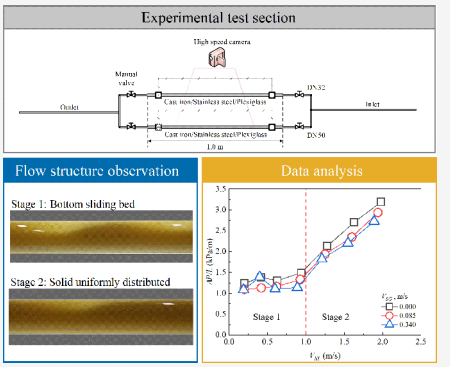

1. INTRODUCTION

Multiphase pipe flows are common in many fields, such as medical science, civil engineering, and fluid mechanics.[1,2] Especially in the field of petroleum engineering, oil and natural gas mixed transportation technology has received extensive attention, and there have been many studies on gas−liquid pipe flows, including pressure pulsation, flow pattern transition, and liquid holdup.[3−6] However, little attention has been given to the apparent wall slip effect of the gas−liquid two-phase flow. Because of the complexity of the multiphase flow system, there is no theoretical support for a comprehensive system thus far. Therefore, existing studies have put more effort into the flow characteristics and paid more attention to the flow domain itself, thus ignoring the interaction between the multiphase fluid and the boundary, which leads to exploration of the wall slip phenomenon in multiphase flow. The phenomenon of wall slip is essentially the apparent relative velocity between the wall and the wall fluid. In fact, "apparent slip" is created by the high-velocity gradient region close to the wall.[7] Evaluating the wall slip effect of a multiphase flow can deeply explore the influence of each phase medium on the flow, the contribution of the wall conditions, and the interaction between the phase and the wall, which could provide ideas for explaining the characteristics of multiphase flow in principle.

Studies have been conducted on the influence of pipe roughness on a two-phase flow. However, no systematic approach considering wall slip phenomena in a gas/liquid two-phase flow has been proposed yet. In addition, sand-bearing crude oil often occurs in the exploitation of sandstone and other reservoirs, and the produced liquid presents a liquid−solid mixed flow in the pipeline. Currently, pipeline flow based on the basic principle of a solid−liquid mixed flow has become an important transportation method in engineering systems. It is of great significance to study the rheological characteristics, flow structure and pressure fluctuation of liquid−solid mixtures for the design and maintenance of transmission pipelines.[8,9] Some scholars have studied the rheological properties of solid−liquid mixtures through experiments and discussed the influence of the solid particle content.[10−13] In contrast to the single-phase flow, the multiphase flow will form different flow patterns and phase distribution structures due to the changes in the phase velocity and fraction, which will lead to a change in the pressure gradient and interphase resistance. With the change in the mixed liquid velocity, the pipe flow of the liquid−solid mixture presents the following flow patterns: a homogeneous flow, a heterogeneous flow, a heterogeneous flow with a sliding bed at the bottom, and a heterogeneous flow with a fixed bed at the bottom. It has been found that when the liquid−solid flow is homogeneous, there are two types of constitutive models for Newtonian and non-Newtonian fluids under different solid volume fractions.[14−16]

Received: December 7, 2021
Revised: March 12, 2022
Accepted: March 16, 2022
Published: March 31, 2022

https://doi.org/10.1021/acs.iecr.1c04797
Ind. Eng. Chem. Res. 2022, 61, 4951−4970

Currently, the measurements of multiphase flows mainly focus on process parameters, such as liquid velocity, volume flow rate, and phase fraction. Accurate monitoring of flow parameters in pipelines is very important for automatic operation and low energy consumption.[17,18] Researchers have studied the flow characteristics of liquid−solid mixtures in pipelines through experiments and established a flow model based on the experimental data of solid particles. Most existing research focuses on the shape, average size, and other parameters of solid particles, and also discusses their influence on the flow characteristics of solid−liquid mixtures while ignoring the effects of flow velocity, pipe size, and wall roughness.[19−22] Moreover, oil exploitation is often accompanied by the production of natural gases. Research on gas−liquid two-phase pipe flow based on this background is quite mature, and a variety of flow parameter testing technologies have been developed to study the conventional gas−liquid two-phase flow pattern conversion, pressure fluctuation, and phase distribution.[23−26] With the development of unconventional resources in the petroleum industry, research on the flow law of multiphase in pipelines has gradually become an important research topic. It is therefore very important to study the critical parameters of the flow pattern transition under different flow conditions. In the study of transport critical conditions, there have been many research results for different media properties. One of the important research results is the predictive model of particle transport velocity under different liquid viscosities in horizontal and inclined pipes given by Archibong Archibong-Eso et al.[27] In gas−liquid flow, significant progress has been made in the study of solid particle transport.[28,29] Previous studies have focused on the influencing factors of solid transport, established the particle transport velocity model, and determined the critical conditions of continuous transport.[30,31]

However, unlike common gas−solid and liquid−solid flows, the gas−liquid−solid coupling flow is more complicated. The change in the flow velocity of each phase affects the flow pattern, especially the behavior of the solid particles. Because the flow characteristics of the three-phase mixture are still uncertain, it is necessary to obtain useful experimental data and establish a general model in order to describe this type of flow.[32] When the influence of pipeline conditions and flow conditions on medium transportation are considered, the liquid−solid mixture could be regarded as a liquid phase. The analysis of pressure loss and influencing factors of the coupling flow in pipelines has received an increasing amount of attention after gas was introduced. Meanwhile, to better explore the theory of multiphase flow, some studies have adopted experimental means to measure the pressure gradient combined with rheometer testing and have determined that there is an apparent wall slip in the process of pipe flow. The flow behavior characteristics and apparent wall slip/depletion phenomenon have been extensively studied for the single liquid phase, gas−liquid two phase, and liquid−solid mixed circular pipe flows.[18,33−35] Studies have determined that the pipe roughness has a significant impact on the apparent wall slip,[36−42] but the influence of the phase fraction and velocity on the apparent wall slip cannot be ignored. Notably, relevant research on the apparent wall slip of gas/liquid−solid mixed pipe flows is still rare. Gas and solid particles exist simultaneously in the pipeline, and the law of the apparent wall slip effect under different flow conditions needs to be further explored.

Thus, the main objective of this study was to evaluate the flow behavior and apparent wall slip (wall depletion) phenomenon for a gas/liquid−solid mixture piping flow based on the gas−liquid and liquid−solid two-phase treatment analogy, and to consider the influence of each phase coupling and pipeline condition on the flow characteristics in a comprehensive manner. It can also provide theoretical guidance for adjusting the driving force and safety monitoring of multiphase-flow pipeline transportation in the petroleum industry.

2. THEORETICAL BACKGROUND

For any flow in the pipe, the apparent shear rate can be estimated by using superficial liquid velocity. Following an analogy with a single-phase treatment, it must be noted that the wall shear stress, τ_w, in these equations must be considered as an overall average value for the liquid−solid mixture flow pressure gradient. Equation 1 can reflect the effective shear rate of the pipe flow of friction loss in the laminar flow process of Newtonian fluids.

$$\dot{\gamma} = 8V_{SL} / D \tag{1}$$

$$\tau_w = \Delta PD / 4L \tag{2}$$

where V_{SL} is the liquid superficial velocity, $\dot{\gamma}$ is the shear rate, $\Delta P/L$ is the pressure gradient, D is the pipe diameter, and τ_w is the wall shear stress.

For the steady-state laminar flow of a non-Newtonian fluid in a circular tube, when there is a wall slip phenomenon, the volume flow rate can be written as follows

$$Q = \pi V_S R^2 + \pi \int_0^R r^2 f(\tau) \mathrm{d}\tau \tag{3}$$

where Q is the volume flow rate, R is the pipe radius, $f(\tau) = -\mathrm{d}u/\mathrm{d}r$ is the constitutive relationship of the time-independent fluid, and V_S is the apparent slip velocity.

Substituting $r = R\tau/\tau_w$ into Equation 3, the following relational expression is obtained:

$$Q = \pi V_S R^2 + \left(\pi R^3 \int_0^{\tau_w} \tau^2 f(\tau) \mathrm{d}\tau\right) / {\tau_w}^3 \tag{4}$$

In the study of wall slip flow characteristics, researchers usually measure the apparent wall slip coefficient by changing the size of the test tool. The apparent wall slip coefficient model was derived based on experimental test data, and the slip velocity was obtained. This method was mainly developed based on the Mooney equation.[43] The continuous equation is expressed as follows

$$8V_{SL} / D = 8V_S / D + \left(4 \int_0^{\tau_w} {\tau_{rx}}^2 \dot{\gamma} \mathrm{d}\tau_{rx}\right) / {\tau_w}^3 \tag{5}$$

In this study, it is assumed that the liquid−solid mixture is uniformly mixed in the main flow area of the pipeline, and that the flow characteristics of the mixture can be expressed as a single-valued function of the shear stress and shear rate. In the process of multiphase flow, the apparent wall slip is mainly due to liquid wetting of the pipe wall. The liquid phase velocity was used instead of the average velocity of the single-phase flow. Therefore, Equation 5 can be applied to this study.

Delgado et al. found in their study of the slip characteristics of grease on the wall surface that the relative roughness of the pipe has a significant influence on the slip velocity.[33] The apparent slip velocity calculation formula is expressed as follows

$$V_S = \frac{C_D \tau_w}{\varepsilon / D} \tag{6}$$

https://doi.org/10.1021/acs.iecr.1c04797
Ind. Eng. Chem. Res. 2022, 61, 4951−4970

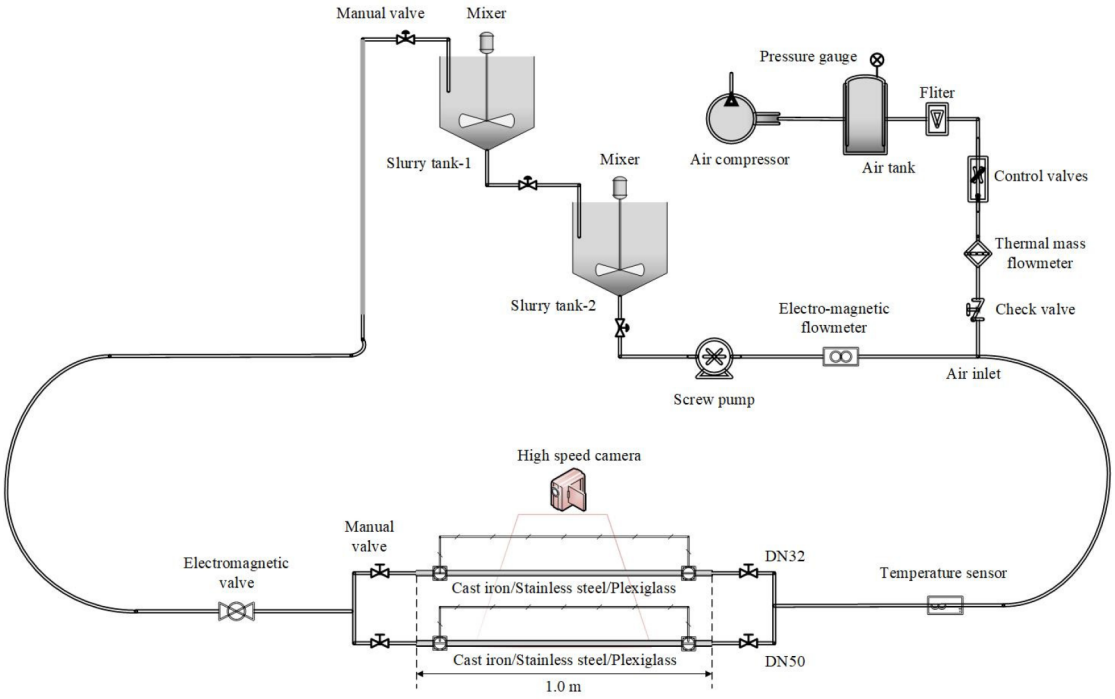

Figure 1. Schematic of the test loop.

where ε is the absolute roughness of the pipe, ε/D represents the relative roughness of the pipe and C_D is the apparent wall slip coefficient. Substituting Equation 6 into the continuous equation, we can obtain Equation 7, and the apparent wall slip coefficient C_D can be estimated at each wall stress value from the slope of these plots.

$$(8V_{SL}/D)/\tau_w = 8C_D/\varepsilon + \left(4\int_0^{\tau_w} \tau_{rx}^{\ 2}\dot{\gamma}d\tau_{rx}\right)/\tau_w^{\ 4} \tag{7}$$

The modified mixing velocity expression was then used to analyze the apparent wall slip effect in a multiphase flow. In a horizontal pipeline, due to the high density of solid particles, the following performance near the wall is relatively poor, which shows that the direction of the slip velocity is opposite that of the mixed flow velocity. Therefore, assuming no apparent wall slip, the modified apparent velocity of the mixture is expressed as follows[33]

$$(V_{SL})_C = V_{SL} - V_S \tag{8}$$

And the corresponding corrected shear rate is as follows

$$(8V_{SL}/D)_C = 8(V_{SL} - V_S)/D \tag{9}$$

where $(V_{SL})_C$ and $(8V_{SL}/D)_C$ represent the corrected slip velocity and corrected shear rate, respectively.

In theoretical research, the Lockhart−Martenelli parameter applicable to any flow pattern is generally used to compare the pressure gradient of multiphase flow and single liquid phase flow in a pipeline. The expression is as follows

$$\Phi_L^{\ 2} = \frac{\Delta P/L}{\Delta P_L/L} \tag{10}$$

where Φ_L represents the Lockhart−Martenelli parameter, $\Delta P/L$ is the multiphase flow pressure gradient, and $\Delta P_L/L$ is the pressure gradient for a liquid flowing alone at the same superficial velocity as in the multiphase mixture. The pressure gradient can be written as follows

$$\Delta P/L = 2f_M V_M^{\ 2}\rho_M/D \tag{11}$$

$$\Delta P_L/L = 2f_L V_{SL}^{\ 2}\rho_L/D \tag{12}$$

where V represents the superficial velocity, ρ is the density, and f is the Fanning friction factor. The subscripts M and L denote the mixed fluid and separate liquid phases, respectively. The mixture velocity can be calculated by the sum of the superficial liquid velocity and the superficial gas velocity, $V_M = V_{SL} + V_{SG}$. The liquid friction factor can be expressed as follows

$$f_L = C_L Re_L^{\ -n} \tag{13}$$

where $C_L = 16$, $n = 1$ for a laminar flow, $C_L = 0.046$, $n = 0.2$ for a turbulent flow, and Re_L represents the liquid Reynolds number. For the liquid phase of a Newtonian fluid, the Reynolds number expression is given as follows

$$Re_L = \frac{\rho_L V_{SL} D}{\mu_L} \tag{14}$$

In addition, with the generalized Reynolds number definition in a multiphase flow system, the mixture Reynolds number can be expressed as follows

$$Re_M = \frac{\rho_M V_M D}{\mu_M} \tag{15}$$

where ρ_M and μ_M represent the mixture density and mixture viscosity of the multiphase flow system, respectively, which can be calculated by the volume fraction of each phase and used to determine the flow state in the pipeline.

For gas−liquid−solid multiphase flow, the volume content of the solid phase in this study is less than 3%, and the particle size is between 125 and 178 μm. When the liquid and solid are fully

https://doi.org/10.1021/acs.iecr.1c04797
Ind. Eng. Chem. Res. 2022, 61, 4951−4970

mixed and developed into a homogeneous flow, the mixture liquid can be regarded as a non-Newtonian fluid phase. For gas/non-Newtonian fluid two-phase pipe flow, the generalized Reynolds number is widely used in the research.[44,45]

The density of the multiphase flowing mixture is calculated according to the volume fraction of the dispersed phase. For gas−liquid two-phase flow, the mixture density is calculated as follows

$$\rho_M = \rho_G \alpha_G + \rho_L (1 - \alpha_G) \tag{16}$$

where α_G is the volume fraction of the gas phase, which can be calculated according to the proportion of the superficial gas velocity, and ρ_G, ρ_L represent the densities of the gas phase and liquid phase, respectively. In addition, when there is gas/liquid−solid mixed multiphase flow in the pipeline, the density of the liquid−solid mixture ρ_{LM} can be used to replace the liquid density ρ_L.

For gas−liquid two-phase flow, the calculation of the mixture viscosity adopts the model proposed by Bankoff, and the formula is as follows

$$\mu_M = \mu_L (1 - \alpha_G) + \mu_G \alpha_G \tag{17}$$

where μ_L is the liquid viscosity. When there is gas/liquid−solid mixed multiphase flow in the pipeline, the viscosity of the liquid−solid mixture μ_{LM} can be used to replace the liquid viscosity μ_L.

Combining Equations 2, 6, and 11, the functional relationship between the mixed friction coefficient and slip velocity can be obtained as follows

$$f_M = \frac{2V_S \varepsilon / D}{C_D V_M^2 \rho_M} \tag{18}$$

The relationship between the Lockhart−Martenelli parameter and the slip velocity can be obtained as

$$\Phi_L^2 = \frac{2V_S \varepsilon / D}{C_D V_{SL}^2 \rho_L f_L} \tag{19}$$

3. EXPERIMENTAL PROCEDURE

3.1. Experimental Setup and Materials. A multiphase flow test loop system was established to simulate the multiphase flow in a pipeline, and a schematic of the test loop is shown in Figure 1. The system can be used to simulate a gas−liquid flow, a liquid−solid flow, and a gas−liquid−solid mixed flow. The test platform consists of power, mixing, pipeline, data testing, and data acquisition systems. The power system provides a stable medium flow for the experimental simulation, which mainly includes two parts: an air compressor and a mortar pump. During the experiment, in order to mix the liquid−solid mixture fully and avoid deposition of solid particles in the mixing tank, a two-stage mixing system was installed in the experimental test system, and a double-layer mixing blade was set inside.

The objective of this work is to investigate the flow behavior of liquid−solid mixtures in pipes with varying roughness values and the effect of gas on the flow. The pipe flow experiment was performed using industrial hydraulic oil, sand particles, and air. The density of the selected hydraulic oil was 828 kg/m^3, and the zero shear rate viscosity was 100.5 mPa·s at 20 °C. A sand sample with a density of 2391 kg/m^3 and a particle size of 125−178 μm was used to prepare the mixture with different volume fractions. The sand fractions in the oil−sand mixture were 0%, 0.7%, 2.0%, and 3.0%, respectively. In addition, the density of air at 20 °C is 1.205 kg/m^3, and the viscosity is 0.0176 mPa·s. To study the relationship between the flow characteristics and pipe conditions, experiments on the horizontal pipe flow were performed with 32 mm and 50 mm pipe diameters and three different materials: polymethyl methacrylate (PMMA), stainless steel, and gray cast iron. The corresponding wall absolute roughness values were 0.01, 0.30, and 1.00 mm, respectively, and the distance between the two pressure taps was 1.0 m. The length of each section was 1.0 m, as shown in Figure 1.

The parameters measured in the pipe flow experiment include the superficial gas velocity, superficial liquid velocity, flow pressure gradient, flow pattern, and liquid phase rheological parameters. Table 1 gives a list of instruments. The measurement parameters correspond to a complete set of data acquisition and control systems, in which the superficial liquid velocity is measured by controlling the electromagnetic flowmeter, and the gas is controlled by adjusting the control valve of the rotameter. In addition, the pressure value in the pipe flow was measured using Honeywell 40PC100G2A pressure sensors. The rheological properties of the liquid phase were measured using a HAAKE RS6000 rotary rheometer. Three repeated experiments were performed under each working condition, and the data used in this work are the average value.

Table 1. List of Instruments

measurement parameters	measuring equipment	measurement range	uncertainty
superficial liquid velocity, V_{SL}	electromagnetic flowmeter (KROHN OPTIFLUX4300C)	0−12 m/s	0.2%
superficial gas velocity, V_{SG}	rotameter	0−5 m/s	1.5%
pressure gradient, ΔP	pressure sensor (Honeywell 40PC100G2A) data acquisition equipment (NI6210)	0−689 kPa	0.15%

3.2. Test Matrices. Most existing research focuses on gas−liquid mixture flows. In this work, the liquid−solid mixed flow and gas/liquid−solid mixed horizontal pipe flow were also tested. The experiment covers a variety of experimental conditions, such as varying pipeline diameters, wall surface roughness, and solid phase volume fractions. Thus, the influencing factors of multiphase flow characteristics in the pipeline can be discussed more comprehensively. Through Reynolds number calculations, it is obvious that the gas−liquid, liquid−solid and gas−liquid−solid mixed flows formed by the flow conditions involved in this work are laminar flows. Table 2 presents the experimental test matrix for the tests conducted on the multiphase flow system, and lists the flow parameters of multiphase flow. According to the generalized Reynolds number calculation formula, the value range of the Reynolds number is estimated, and the results show that the multiphase flow in this work is in a laminar state.

4. RESULTS AND DISCUSSION

In a multiphase flow system, gas−liquid−solid phases are coupled in the pipeline, and the property parameters of the gas, liquid, and solid particles will lead to the formation of unique flow behavior characteristics. The pressure loss and apparent wall slip effect in the pipe flow are important factors that affect the change in the liquid holdup of the multiphase flow, and they are also important for explaining the flow structures.

https://doi.org/10.1021/acs.iecr.1c04797
Ind. Eng. Chem. Res. 2022, 61, 4951−4970

Table 2. Experimental Test Matrix

flow composition	superficial liquid velocity, V_{SL} (m/s)	superficial liquid velocity, V_{SG} (m/s)	solid volume fraction, C_V (%)	gas volume fraction, α (%)	mixture density, ρ_M (kg/m^3)	mixture velocity, V_M (m/s)	mixture viscosity, μ_M (Pa·s)	generalized Reynolds number, Re_M	flow type
gas−liquid two-phase flow	0.07−3.76	0−0.82	0	1.9−13	≤828	≤4.47	0.017−0.1005	≤2254	laminar flow
liquid−solid flow	0.16−1.98	0	0.7, 2, 3	0	≤875	≤3.93	0.085−0.109	≤1019	laminar flow
gas/liquid−solid flow	0.16−1.84	0−0.34	0.7, 2, 3	2.0−18	<875	≤3.93	0.085−0.109	≤2087	laminar flow

During data analysis, the measurement error of the parameters and the error propagation of the derived function are comprehensively evaluated. According to error propagation proposed by Bevington and Roinson,[46] an error transfer analysis is performed on the indirect measurement parameters derived from the direct measurement parameters in the study.

Suppose the indirect measurement parameter is $f = f(x,y, ..., n)$; the error propagation formula is then defined as follows

$$\sigma_f = \sqrt{\sigma_x^2\left(\frac{\partial f}{\partial x}\right)^2 + \sigma_y^2\left(\frac{\partial f}{\partial y}\right)^2 + ... + \sigma_n^2\left(\frac{\partial f}{\partial n}\right)^2} \quad (20)$$

where σ_f is the error of the indirectly measured parameter, and $\sigma_x,\sigma_y,\cdots, \sigma_n$ represent the error of the direct measurement parameters x and y of the component parameter f, respectively. It should be noted that the error of the direct measurement parameters is calculated by the standard error of the average value:

$$\sigma_{x,y,...,n} = \sqrt{\frac{\sum_{i=1}^{N}(x_i - \bar{x})^2}{N(N-1)}} \quad (21)$$

where N represents the number of standard repeated experiments.

4.1. Flow Behavior of Gas−Liquid Two-Phase Flow.

4.1.1. Experimental Pressure Gradient. The air/hydraulic oil mixture flows along pipes with diameters of 32 and 50 mm at different liquid phase velocities. The inner surface of the pipe has three roughness conditions. The original data of the two-phase flow pressure gradient measured in the experiment are shown in Figure 2.

This indicates that the pressure gradient of the gas−liquid two-phase flow increases with an increase in the superficial liquid velocity. However, air injection significantly increases the pressure gradient reduction. As can be observed, for the same superficial velocity of gas and liquid, the flow pressure gradients in the pipeline with a high relative roughness are higher than those in the smooth pipeline. In addition, the effect of the pipe wall roughness on the gas−liquid flow is obvious under the condition of a high superficial liquid velocity, while the flow difference caused by roughness is not obvious at low liquid velocities. It should be noted that by comparing the pressure gradient difference between the two pipe diameters in Figure 2a,b, the pressure loss of the small-diameter pipe is obviously higher than that of the large pipe at the same gas and liquid velocities. This is because the flow structure with a small diameter is more likely to form a strong turbulence flow or transition flow, resulting in a larger pressure gradient.

In the gas−liquid pipe flow experiment, the maximum superficial liquid velocity is 3.76 m/s, and the superficial gas velocity is controlled at 0−0.82 m/s. By calculating the mixture Reynolds number corresponding to different pipe diameters, we

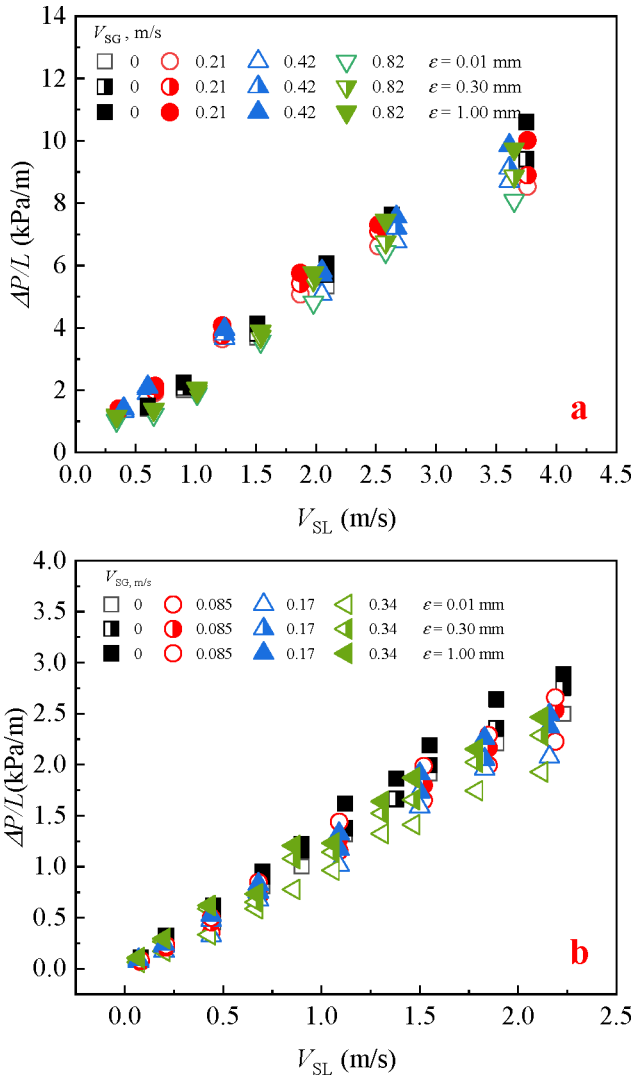

Figure 2. Pressure gradient variation in a gas−liquid two-phase pipe flow: (a) pipe diameter of 32 mm; (b) pipe diameter of 50 mm.

identify the maximum value as 2254, and it is considered that the gas/liquid two-phase flow is still laminar under the experimental conditions of this study. Therefore, this work uses the basic assumption of laminar flow to calculate the effective shear rate and wall shear stress and further discusses the phenomenon of the apparent wall slip. Figure 3 shows the changing trend of the pressure gradient of the two-phase flow with the mixture's Reynolds number. When the superficial gas velocity is constant, the increase in the superficial liquid velocity leads to an increase in the velocity of the two-phase mixture, and the volume fraction ratio of the liquid phase to the gas phase increases, resulting in an increase in the Reynolds number of the mixture. The figure

https://doi.org/10.1021/acs.iecr.1c04797
Ind. Eng. Chem. Res. 2022, 61, 4951−4970

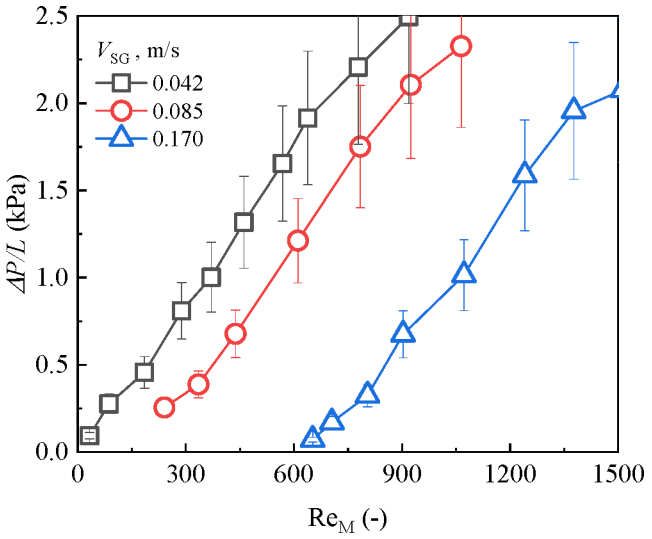

Figure 3. Pressure gradient of gas−liquid two-phase flow varies with the mixture's Reynolds number.

shows that with an increasing Reynolds number, the pressure gradient tends to increase significantly, and the superficial gas velocity has a significant influence on the Reynolds number, which in turn affects the pressure gradient.

4.1.2. Apparent Wall Slip in Gas/Liquid Two-Phase Flow. Under the same pipe diameter and flow conditions, the different pipe roughness values have a significant impact on the flow curve, as shown in Figure 4. The pressure gradient of gas−liquid flow in the rough pipeline is obviously higher than that in the smooth pipeline, and the difference is more obvious at higher shear rates.

In the experimental study, the influence of the pipe scale effect on the gas−liquid flow was explored. Figure 5 shows the variation law of shear stress with the shear rate obtained from the test of PMMA pipes (the absolute roughness value is 0.30 mm) with different diameters. The inner diameters of the corresponding pipes were 32 and 50 mm, respectively. It can be observed from the figure that the flow curves obtained from the test of two pipes with different pipe diameters are almost the same; that is, the slip velocity is not affected by the pipe diameter, which is mainly related to the relative roughness of the pipe wall. This result is in good agreement with that of Delgado et al.[33]

The apparent wall slip velocity can be obtained by combining the theoretical research formula and pressure gradient data. The experimental data show that there is a linear relationship between $(8V_{SL}/D)/\tau_w$ and $1/\varepsilon$, and its slope is an integral multiple of the wall slip coefficient (Equation 7). Then, the wall slip coefficient is introduced into Equation 6 to solve the apparent wall slip velocity.

As shown in Figure 6, the gas velocity has a significant effect on the wall slip in the gas−liquid two-phase flow. As the apparent velocity of the gas phase increased, the slip velocity showed an increasing trend. The increase in the gas superficial velocity then leads to an increase in the linear velocity of the gas−liquid mixture and an increase in the slip effect, which weakens the effect of gas occupying the pipe wall. Therefore, the slip velocity is positively correlated with the gas velocity. This finding is valid under different wall shear stress conditions. With an increase in the wall shear stress, the slip speed increased significantly. Figure 7 shows the variation in the relative slip

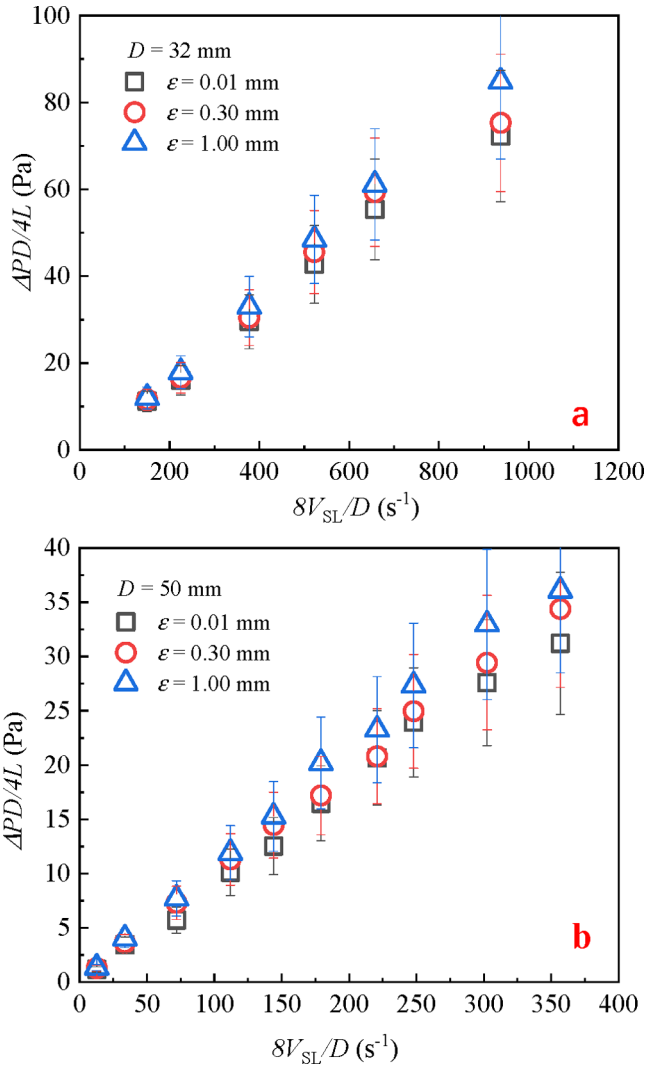

Figure 4. Flow curves of gas−liquid two-phase pipe flow: (a) pipe diameter of 32 mm, (b) pipe diameter of 50 mm.

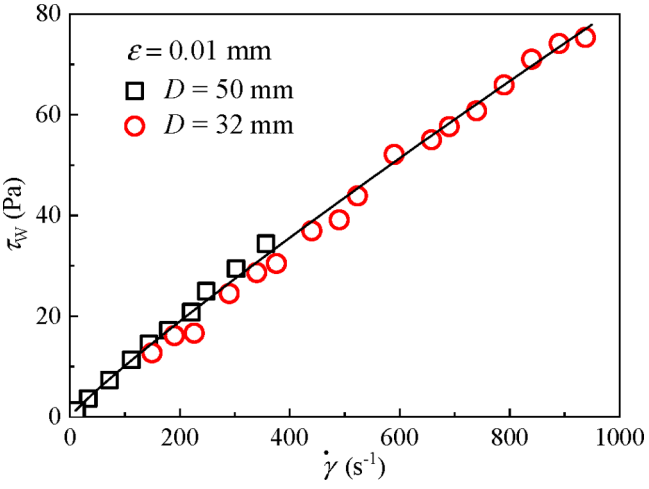

Figure 5. Relationship between the wall shear stress and shear rate under different pipe diameters in gas−liquid pipe flow.

contribution with the apparent gas velocity. Under the same pipeline conditions, in the gas−liquid two-phase flow, the increase in the apparent gas velocity leads to an increase in the

https://doi.org/10.1021/acs.iecr.1c04797
Ind. Eng. Chem. Res. 2022, 61, 4951−4970

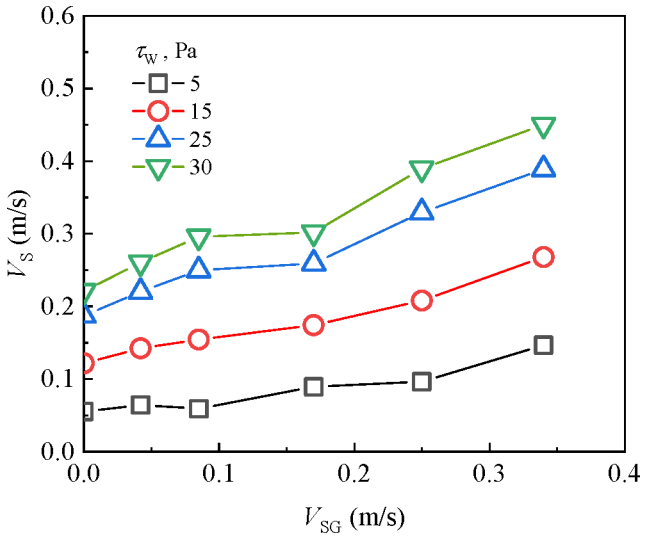

Figure 6. Relationship between the wall slip velocity and gas superficial velocity in gas–liquid pipe flow.

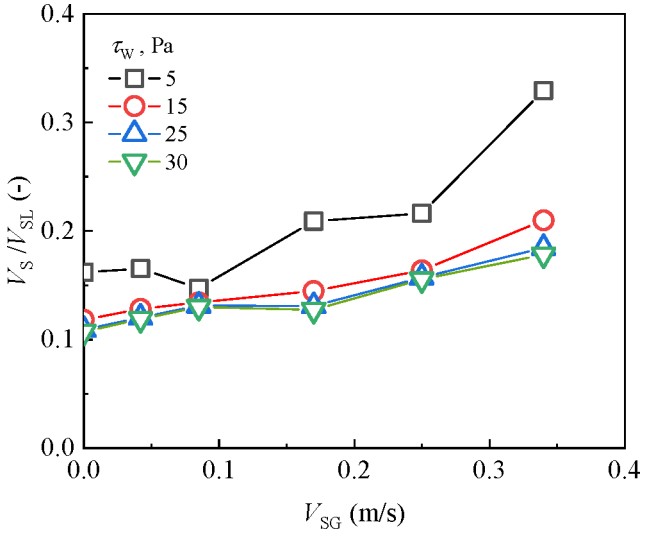

Figure 7. Relationship between the relative slip contribution and gas volume fraction in gas–liquid pipe flow.

relative slip contribution, indicating that the gas promotes slippage in the pipeline. However, when the pipeline forms a steady flow under a high shear stress, there is little difference in the slip contribution rate under different wall shear stresses.

4.2. Flow Behavior of the Liquid–Solid Mixture. In the rheological test of the oil–sand mixture, a stirrer was used to ensure that the liquid and solid were fully mixed, and the apparent viscosity of the mixture was measured to determine the constitutive type of the mixed fluid. Rheological tests of oil–sand mixtures with different solid contents were performed (0%, 0.7%, 2%, and 3%). Figure 8 shows that the oil–sand mixture is a shear-thinning fluid, and its apparent viscosity is lower than that of pure hydraulic oil when the volume fraction is less than 3.0%. At a constant shear rate, as the solid volume fraction increased, the apparent viscosity first decreased and then increased. This shows that adding a small amount of sand to pure hydraulic oil can have a certain drag reduction effect, but if the volume fraction of the sand continues to increase, the apparent viscosity of the mixture increases.

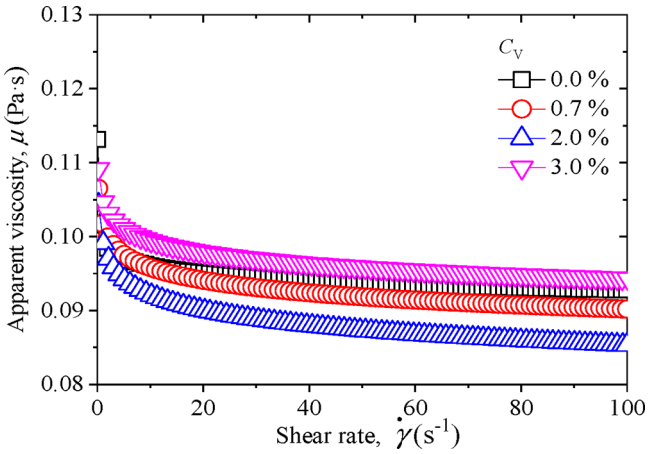

Figure 8. Viscosity curve of oil–sand mixtures under different volume concentrations.

In the actual transportation process of a liquid–solid mixture, if the transportation speed is low, then solid deposition can easily occur at the bottom of the pipeline. However, with an increase in the transport velocity, the solid deposition at the bottom decreases gradually, and the corresponding velocity is the critical transport velocity when the sediment disappears. To ensure conveying efficiency, it is necessary to ensure that the conveying speed is higher than the critical speed. However, if the conveying speed is too high, a greater energy dissipation will occur, which will reduce the conveying efficiency. Next, by analyzing the results of the liquid–solid mixed liquid pipeline flow experiment, we discuss the variation in the pressure gradient and the critical velocity range of the mixed fluid flowing in pipelines with varying wall roughness values, and the influence of pipeline conditions and solid particles on the flow is further studied in this work.

4.2.1. Pressure Gradient and Flow Structure. The selected experimental liquid–solid mixture pressure gradient raw data are shown in Figure 9. Under the same pipe roughness, the concentration of solid particles had a significant effect on the pressure gradient. When there are no solid particles in a single oil flow, the pressure gradient has a good positive proportional relationship with the liquid velocity. However, the addition of

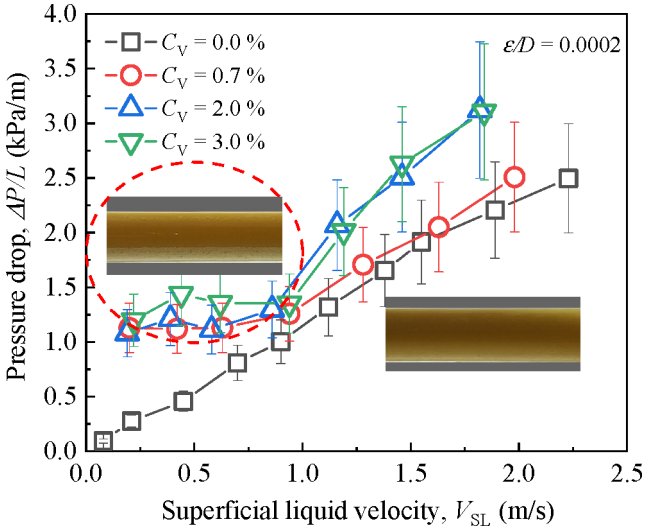

Figure 9. Effect of the solid volume fraction on the pressure gradient in liquid/solid flow.

https://doi.org/10.1021/acs.iecr.1c04797
Ind. Eng. Chem. Res. 2022, 61, 4951–4970

solid particles changed the above linear relationship. The pressure gradient of the mixed liquid was almost constant at a small superficial velocity of the mixed liquid. This is because under the condition of a low superficial velocity, the liquid−solid mixture has not yet reached the full start-up state, resulting in the deposition of sand particles at the bottom of the pipeline, and the sediment particles at the bottom of the pipeline interact with one another. At this time, the solid particles deposited at the bottom of the pipeline only transfer in a small range and cannot be fully mixed with the upper oil phase. However, when the mixing liquid velocity exceeds 1 m/s, the hydraulic pressure gradient of the liquid−solid mixture is similar to that of the pure liquid flow; that is, with an increase in the liquid velocity, the pressure gradient increases gradually. The liquid velocity corresponding to the pressure gradient transition point can be regarded as the critical liquid velocity for stable flow, and the critical velocity for homogeneous liquid−solid flow is between 0.75 and 1 m/s.

The difference in the flow velocity leads to different flow structures, and the transition of the flow regime is often divided by the critical liquid phase. Figure 10 shows the change process

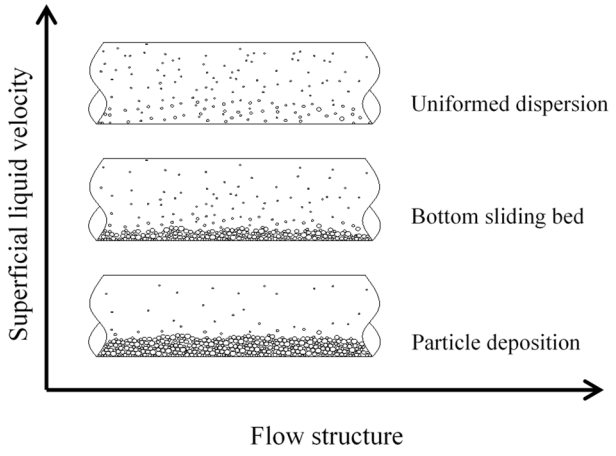

Figure 10. Schematic of the flow structure of the oil−sand mixture.

of the liquid−solid mixed flow structure in a horizontal pipe under different liquid velocities. Combined with the above diagram and the pressure gradient curves shown in Figure 9, the following analysis can be performed: when the flow velocity is lower than the critical flow velocity, the pressure gradient is not obviously affected by the solid volume fraction. However, when it is higher than the critical flow velocity, the solid volume fraction has a significant effect on the flow. This is because when the velocity is lower than the critical velocity, the solid particles are mainly deposited at the bottom of the pipe, while the concentration of suspended particles in the upper liquid is small; therefore, the overall flow pressure gradient is less affected by the solid concentration. However, when the flow rate of the mixture exceeds the critical value, the larger the solid volume fraction is, the greater the friction and collision loss between the solid particles in the flow, which causes the pressure gradient to gradually increase as the solid fraction increases.

In addition, the pressure gradient curve of the 0.7% solid fraction is similar to that of pure oil (solid phase content of 0%) but is significantly different from that of high solid fractions (solid phase content of 2% or 3%) when the liquid flow rate exceeds the critical velocity (as shown in Figure 8). This is because the viscosity of the mixed liquid is smaller than that of pure oil with a small concentration of sand, and the sand particles have a certain filling effect on the rough wall surface, thus forming an oil−sand mixture containing fine sand particles. Figure 11 shows a diagram of a low-viscosity mixed liquid slip

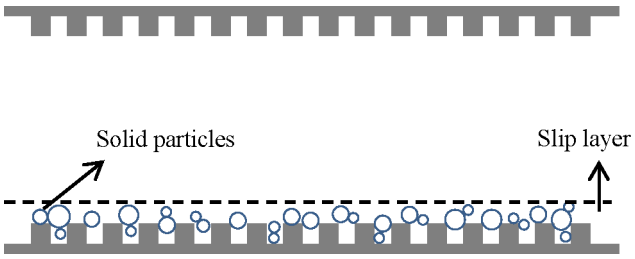

Figure 11. Schematic of the low-viscosity slip layer in the pipeline.

layer near a rough wall. This low-viscosity liquid layer plays a role in lubrication. However, when the solid volume fraction is large, the solid sand grains also play a role in filling the rough pipe wall, but the viscosity of the mixed liquid gradually increases, which results in an interaction between the sand grains and the wall surface. Therefore, there are significant pressure gradients in the pipe flow with high solid volume fractions.

It is worth noting that the pipe conditions are also important factors in studying the flow characteristics of liquid−solid mixed flows. As shown in Figure 12, in the fully developed pipe flow, the pressure gradients in the rough pipes are higher than those in the smooth pipes for the same liquid velocity and solid fraction.

In the liquid−solid mixed flow, the volume content of solid particles is 0.7%, 2%, and 3%. The apparent viscosity range of the liquid−solid mixture is 85.3−109.2 mPa·s, which is obtained from the rheometer test results. The superficial liquid velocity range is 0.16−1.98 m/s, and the maximum mixture Reynolds number is 1019. Therefore, the flow of the liquid−solid mixture in the pipeline can be judged as a laminar flow. The change trend of the pressure gradient with the mixture Reynolds number at different solid phase holdups is shown in Figure 13. When the Reynolds number is small, the pressure gradient does not change significantly, and the macroscopic appearance shows particles deposited at the bottom of the pipeline that have not been completely suspended. However, when the Reynolds number increases to approximately 300, the pressure gradient curve has a breakpoint. With a further increase in the mixture's Reynolds number, the pressure gradient increases significantly. Under the condition of a high solid phase holdup, the pressure gradient increases faster.

Figure 14 shows the influence of the pipe diameter on the flow with and without sand particles. The data points of the single oil phase and oil−sand mixture are represented by hollow data points and semisolid data points, respectively. The influence of the pipe diameter on the flow is not obvious in the single-phase hydraulic oil experiment. In contrast to the single-liquid phase pipe flow, the effect of the pipe size on the flow characteristics cannot be ignored in liquid−solid mixed flows.

At a high solid concentration, different pipe diameters lead to different degrees of deposition of solid particles. The increase in the pipe size makes it easier for sand particles to be deposited at the bottom. Therefore, the interaction between the solid particles and the wall surface is enhanced during the flow process, which results in a higher shear stress and pressure gradient.

https://doi.org/10.1021/acs.iecr.1c04797
Ind. Eng. Chem. Res. 2022, 61, 4951−4970

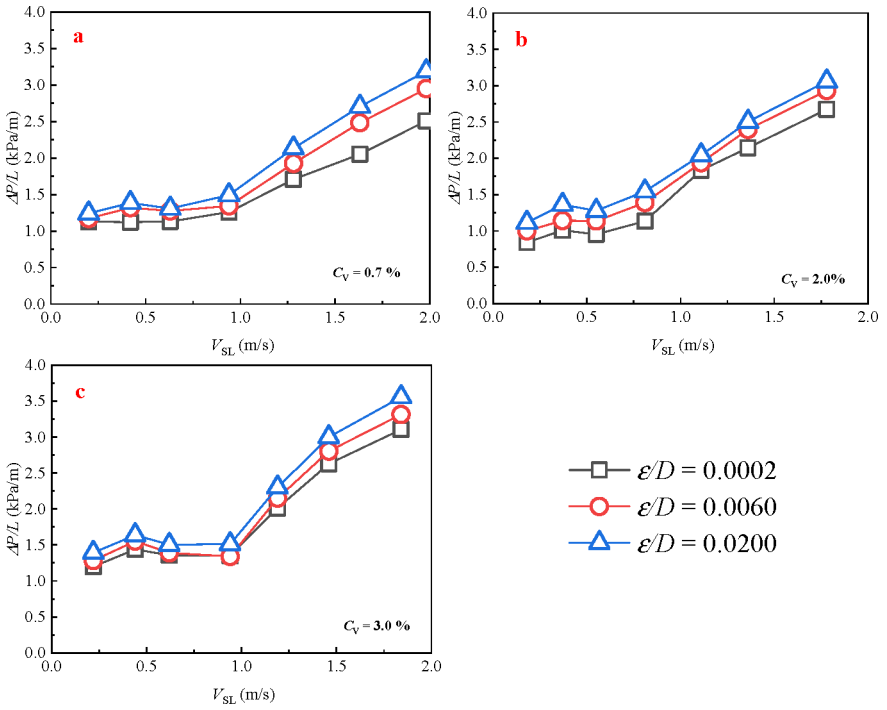

Figure 12. Relationship between superficial liquid velocity and pressure gradient in liquid/solid flow: (a) C_V = 0.7%, (b) C_V = 2.0%, (c) C_V = 3.0%.

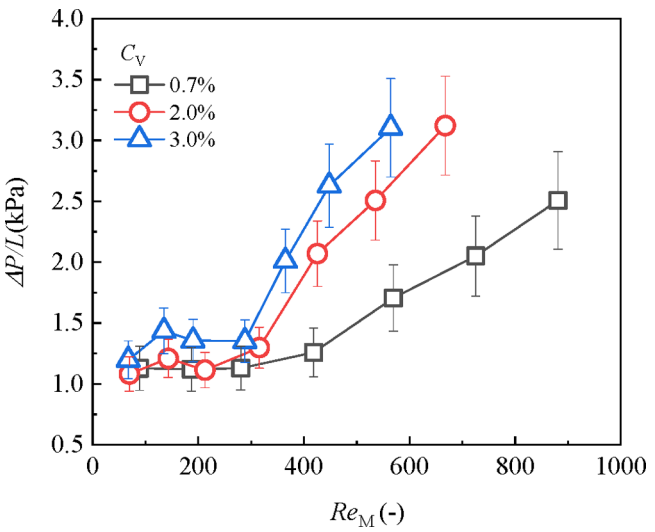

Figure 13. Relationship between the pressure gradient of the liquid/solid mixture and the Reynolds number of the mixture.

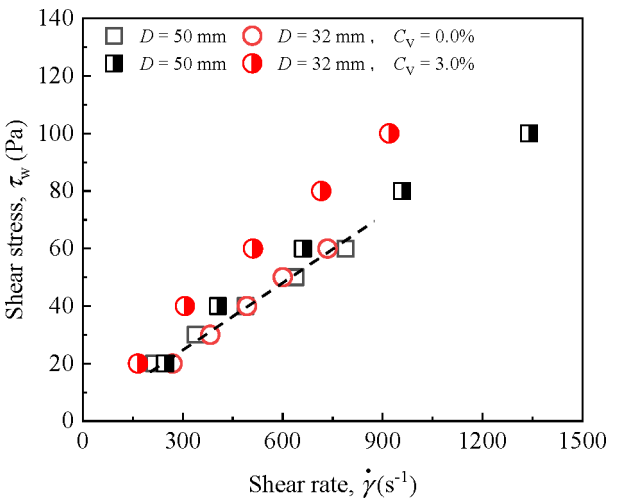

Figure 14. Flow curves of different pipe diameters of the liquid/solid mixture.

4.2.2. Apparent Wall Slip. The shear stress−shear rate relationship curves with different wall surface roughness conditions not only reflect the flow characteristics in the pipe, but also determine whether there is an apparent wall slip. Figure 15 shows the variation in the wall shear stress with the shear rate when the liquid−solid mixture flows in the pipe with a fixed solid volume fraction and pipe diameter. For the same liquid conditions, the rheological characteristic curve should be unique. However, as shown in Figure 13, in a liquid−solid mixed flow, the difference in the pipe roughness leads to different viscosity curves, especially at high shear rates, which also shows that the wall slip phenomenon does exist in the liquid−solid mixture during the flow process.

Figure 15 shows a comparison between the modified flow characteristic data of the liquid−solid mixture and the flow characteristic curve in pipes with varying roughness values. The hollow data points reflect the real mixed flow, while the solid points are the modified flow data without a wall slip, which is calculated based on Equation 9. The results show that the modified data are similar to the pipe flow characteristics under the condition of a large roughness, and it also reflects that the roughness can reduce the apparent wall slip effect in a pipe flow, to a certain extent.

According to Equations 6 and 7, the wall slip velocity of the liquid−solid mixture flow is closely related to the wall relative roughness, solid volume fraction, and wall shear stress. On the basis of the experimental data and equations, the apparent wall slip velocity of the mixed flow of the liquid−solid mixture in a horizontal pipe was calculated. As shown in Figure 16, under the same pipe roughness, the slip velocity was positively correlated with the wall shear stress. When the solid volume fraction in the

https://doi.org/10.1021/acs.iecr.1c04797
Ind. Eng. Chem. Res. 2022, 61, 4951−4970

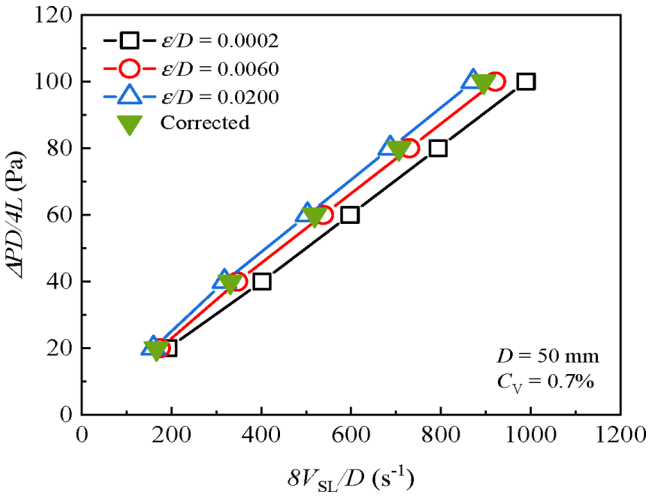

Figure 15. Viscous flow curve of the liquid/solid mixture under different roughness conditions.

mixture liquid was small, the slip velocity was slightly higher than that of the pure oil flow because the lower solid volume fraction filled the inner wall of the pipe to avoid the roughness and form a thinner lubrication layer, which increased the apparent wall slip effect; however, when the solid content continued to increase, the slip velocity gradually decreased and finally stabilized. This occurs because as the volume fraction of solid particles continues to increase, the viscosity of the mixture increases, and the friction loss between the mixture and the pipe wall and between the solid particles themselves increases, so the slip effect will be reduced, which can be easily understood through the collision diagram in Figure 17. Figure 17 shows the collision between solid particles and the pipe wall and the collision between solid particles in the pipe flow, which results in a friction loss. These collisions are random, and the lines show the movement of the particles bouncing off the wall. The enlarged view is a schematic diagram of the collision between solid particles, indicating that the direction of the particle movement is different. Among them, v_1 and v_2 represent the velocity directions of the two particles, but the directions are not fixed. In addition, comparing the slip velocity under the different relative roughness conditions in Figure 16, the results show that with an increase in the pipe roughness, the apparent wall slip velocity of the liquid−solid mixture flow gradually decreases. This conclusion also confirms that the apparent wall slip effect can be weakened by increasing the pipe roughness.

In general, the relative slip contribution is used to express the effect of the apparent wall slip on the flow in pipes,[47] which is expressed as the ratio of the apparent wall slip velocity to the superficial liquid velocity, V_S/V_{SL}. The relationship between the relative slip contribution and the solid volume fraction is shown in Figure 18, which includes four wall shear stresses: 40, 60, 80, and 100 Pa. With an increase in the solid volume fraction, the relative slip contribution first increased to a certain extent and then gradually decreased. When the solid content exceeded 2%, the relative slip contribution increased again with an increase in the solid content. In the studied solid volume fraction, the relative slip contribution of the oil−sand mixture flowing in the PMMA tube was approximately 5%−20%. Therefore, for the flow of the oil−sand mixture in a smooth pipe, the apparent wall slip plays a greater role in the pressure gradient. Under different wall shear stress conditions, the variation trend of the relative slip contribution with the solid content is the same. It can be seen that the wall shear stress has little effect on the relative slip contribution, and when the solid content increases to 3%, the effect of wall shear on the slip contribution ratio can be ignored.

4.3. Flow Characteristics of the Gas/Liquid−Solid Mixture. *4.3.1. Experimental Pressure Gradient.* Gas partic-

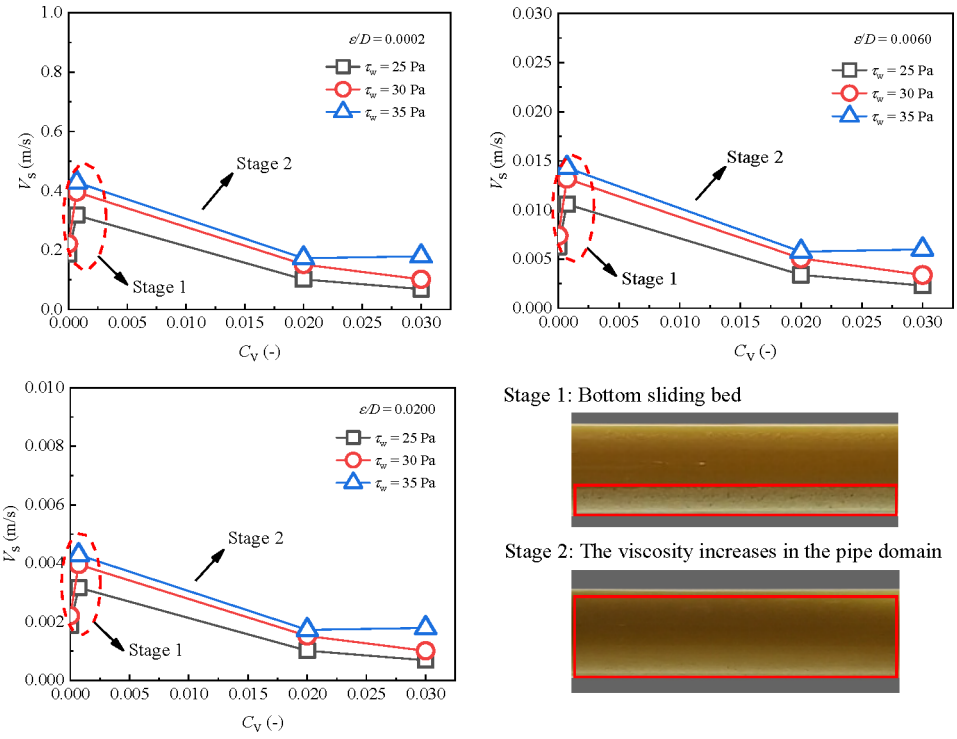

Figure 16. Influence of the solid fraction on the apparent wall slip velocity in liquid/solid pipe flow.

https://doi.org/10.1021/acs.iecr.1c04797
Ind. Eng. Chem. Res. 2022, 61, 4951−4970

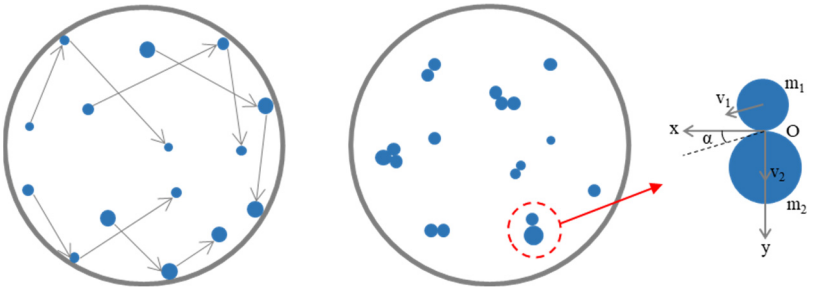

Figure 17. Schematic of the collision between particles and between the particles and the pipe wall.

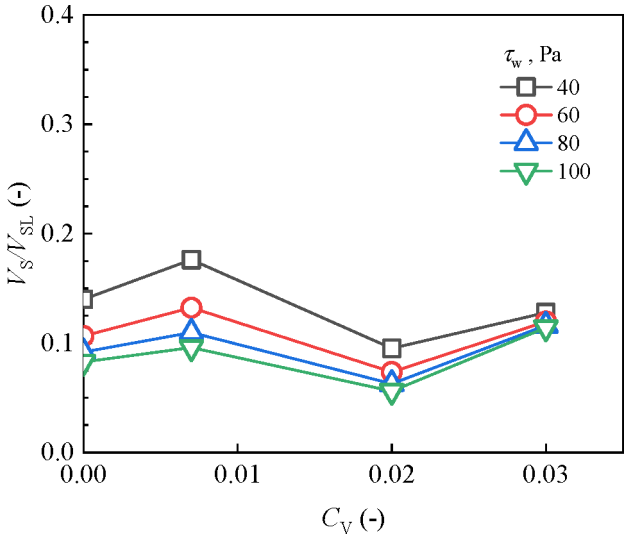

Figure 18. Effect of the solid fraction on the relative slip contribution.

ipation has a significant influence on the flow of the liquid−solid mixture in a horizontal pipeline. Figure 19 shows the relationship between the superficial gas velocity and the flow pressure gradient under the condition of a solid fraction of 0.7%. With an increase in the superficial gas velocity, the experimental pressure gradient decreases, which is more obvious as the liquid flow rate increases. This is because the gas helps form a low-viscosity mixture in the flow and plays a lubricating role. Air injection can dampen the friction loss and significantly reduce the pressure gradient. In addition, similar to liquid−solid flow, mixed flow with gas also has two flow structures. As shown in Figure 19, due to gravity the gas is close to the upper wall of the pipeline. The solid particle deposition at the bottom of the pipeline decreases with an increase in the liquid velocity. The experimental results show that the flow structure from the bottom deposition to uniform development is mainly affected by the superficial liquid velocity, but it is almost independent of the gas (Figure 20). As shown in Figure 19a,b,c, the pressure gradients in a flow in rough pipes are higher than those in smooth pipes for the same gas and liquid flow rates.

When the gas is injected into the liquid−solid mixture, the mixing density and mixing viscosity will change. Estimated with the help of the gas content and incorporated into the generalized Reynolds number definition, the Reynolds number of the gas/

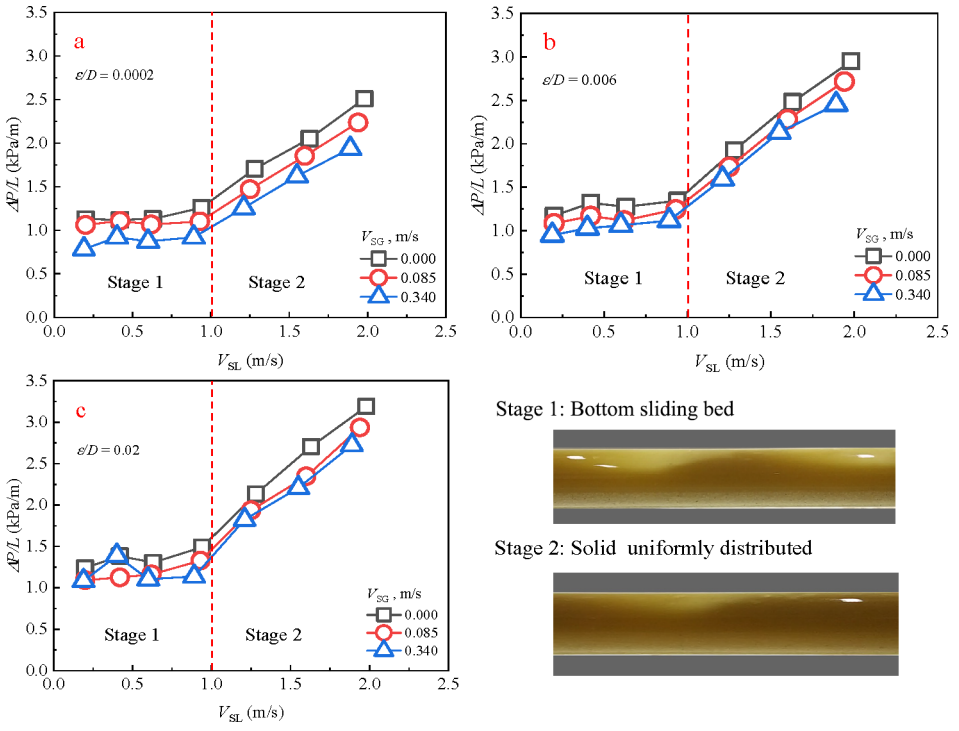

Figure 19. Effect of gas superficial velocity on the flow pressure gradient in gas/liquid−solid flow: (a) $\varepsilon/D = 0.0002$, (b) $\varepsilon/D = 0.006$, (c) $\varepsilon/D = 0.02$.

https://doi.org/10.1021/acs.iecr.1c04797
Ind. Eng. Chem. Res. 2022, 61, 4951−4970

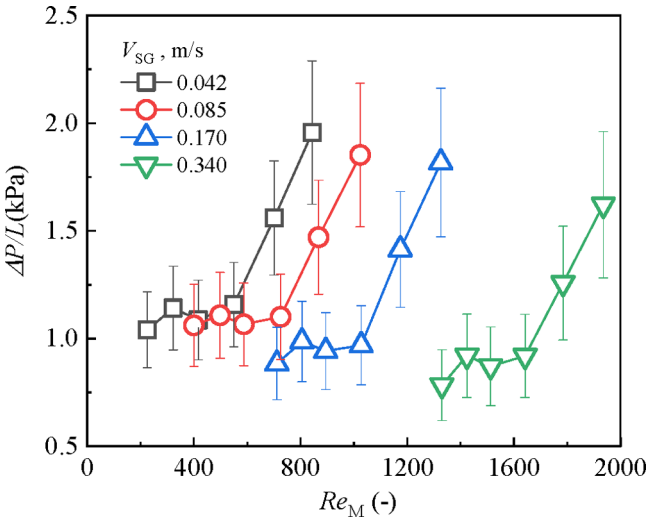

Figure 20. Variation in the pressure gradient with the Reynolds number in the flow of the gas/liquid–solid mixture (C_V = 0.7%).

liquid–solid mixed flow can be solved to be 87-2087. Therefore, the gas/liquid–solid mixed flow can be regarded as a laminar flow in horizontal pipes. Figure 21 presents the effect of the

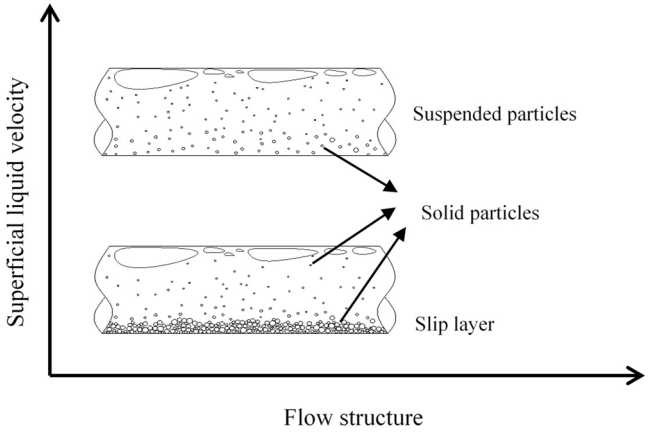

Figure 21. Schematic of the gas/liquid–solid mixed flow structure under fixed gas conditions.

mixture Reynolds number on the pressure gradient under the conditions of a solid phase content of 0.7% and different gas phase velocities. Compared with Figure 13, the gas injection has a significant effect on the flow: on the one hand, it can reduce the viscosity of the mixed liquid, while on the other hand, it can increase the mixture velocity. The increase in the gas velocity leads to an increase in the ratio of the inertial force to the viscous force of the mixture and has a greater impact on the deposition of solid particles.

Figure 22 exhibits the characteristic flow curve of a gas/liquid–solid mixture. Under the condition of a low shear rate, the effects of both the gas and solid fraction on the flow are not obvious. The reason is that the flow is in the start-up stage at this time, and it has not yet reached a steady state, so there is a small difference in the flow characteristics. As the shear rate increases, the pressure gradient increases proportionally. The experimental results show that the critical shear rate of the flow state transition is approximately 150 s^{-1}. When the shear rate exceeds the critical value, a uniform flow is formed in the pipe. As shown in Figure

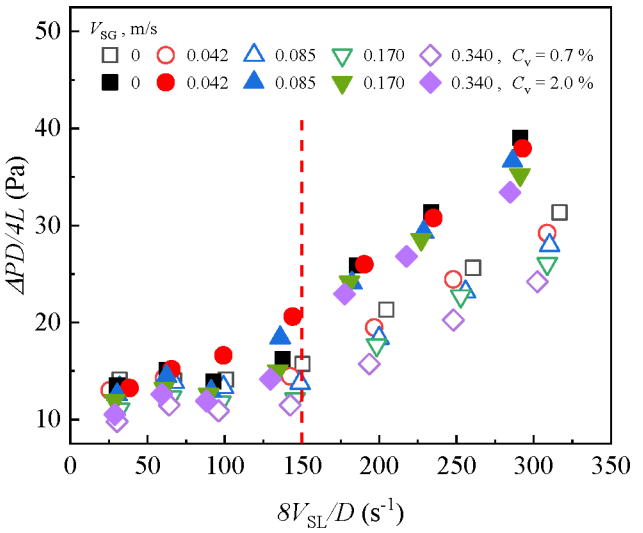

Figure 22. Relationship between the shear stress and shear rate at different superficial gas velocities.

22, the increase in the superficial gas velocity can reduce the wall shear stress.

Moreover, an increase in the solid concentration leads to an increase in the apparent viscosity of the mixture, which indicates an increase in the slope of the stress–strain relationship. Under the condition of a high shear rate, the collision of solid particles and walls as well as particles increases, which causes a loss of energy. Therefore, at the same shear rate, an increase in the solid volume fraction leads to an increase in the shear stress.

These results are also presented in the form of the Lockhart–Martenelli parameter and superficial gas velocity (Figures 23 and

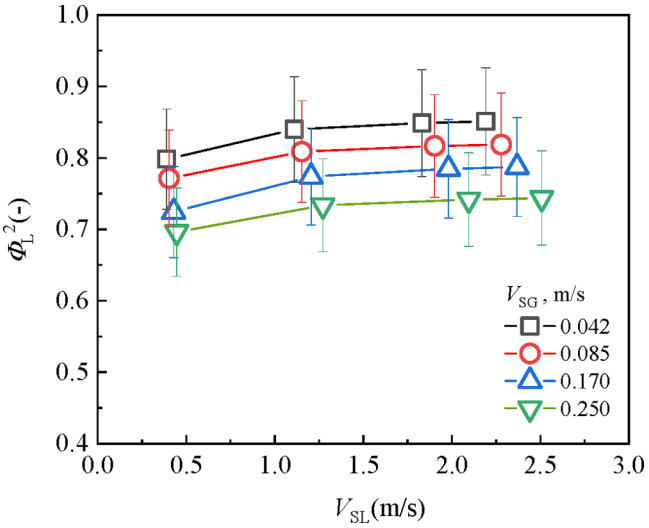

Figure 23. Lockhart–Martenelli parameter as a function of the superficial liquid velocity in gas/liquid–solid flow.

24). The resistance ratio is a dimensionless parameter that facilitates the evaluation of the pressure gradient reduction caused by air or small particle injection in a multiphase flow compared to pure hydraulic oil that flows by itself at the same volume rate. When there is gas–liquid flow in the pipeline and the solid volume fraction is 0, under the condition of a constant gas-phase superficial velocity, the resistance ratio gradually increases with an increase in the liquid superficial velocity. This

https://doi.org/10.1021/acs.iecr.1c04797
Ind. Eng. Chem. Res. 2022, 61, 4951–4970

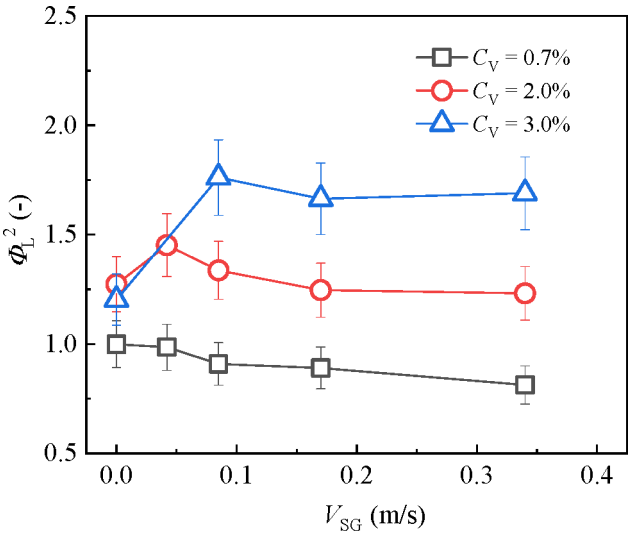

Figure 24. Lockhart–Martenelli parameter for the gas/liquid–solid studied as a function of the superficial gas velocity.

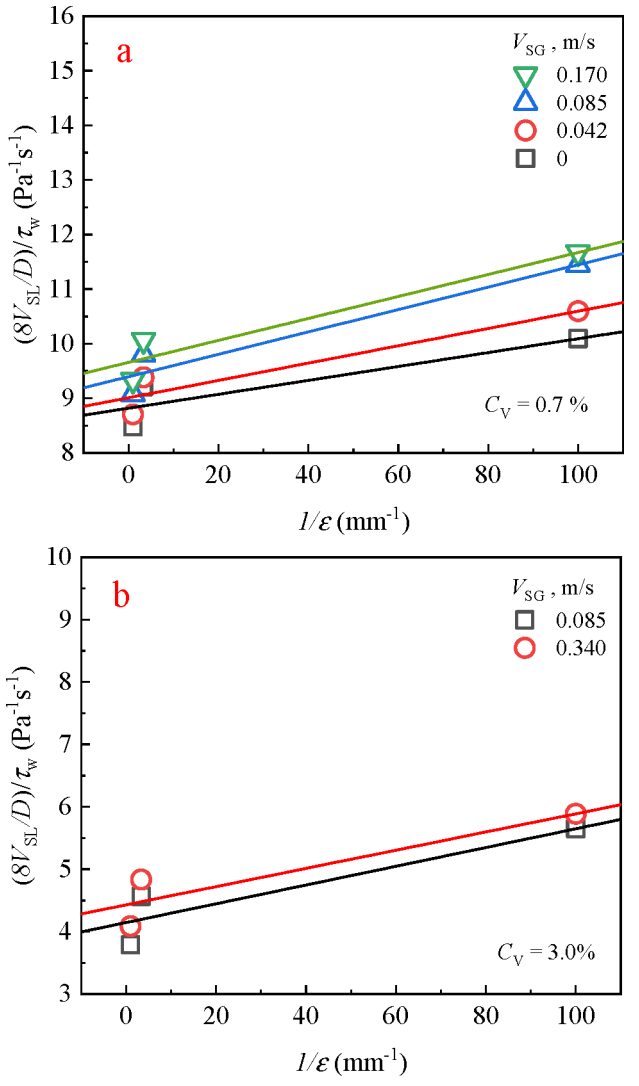

Figure 25. Relationship between $(8\ V_{SL}/D)/\tau_w$ and $1/\varepsilon$: (a) C_V = 0.7%, (b) C_V = 3.0%.

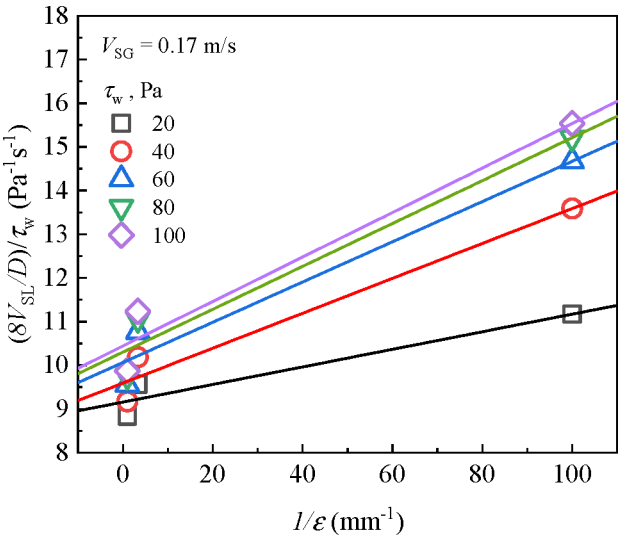

Figure 26. Effect of the wall shear stress on the slip coefficient at a fixed superficial gas velocity in gas/liquid–solid flow.

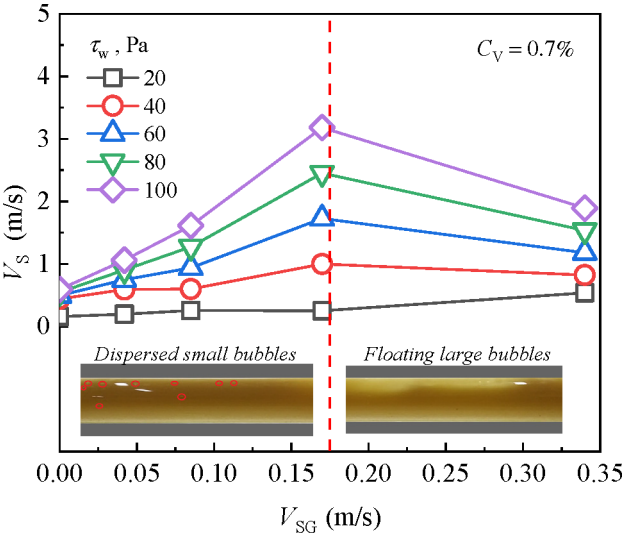

Figure 27. Relationship between the apparent wall slip velocity and superficial gas velocity of gas/liquid–solid flow under different shear stress conditions.

rule behaves similarly with different gas velocities. In addition, the Lockhart–Martenelli parameter is negatively correlated with the superficial gas velocity.

The influence of the presence of solid particles on the flow is shown in Figure 24. When the volume fraction of the solid phase is small, the change trend of the Lockhart–Martenelli parameter values with the superficial gas velocity is similar to that of the gas–liquid two-phase flow; that is, when the gas velocity is 0, the value of the Lockhart–Martenelli parameter approaches 1, while when the gas velocity increases, the Lockhart–Martenelli parameter gradually decreases, and the pressure gradient decreases. However, when the solid volume fraction is large, as the superficial gas velocity increases, the Lockhart–Martenelli parameter coefficient value first increases and then decreases. At this time, the injection of gas starts to promote the uniform dispersion of solid particles in the mixed liquid, resulting in a higher mixture density than that of hydraulic oil alone and an increase in the pressure gradient. When the liquid–solid flow is

https://doi.org/10.1021/acs.iecr.1c04797
Ind. Eng. Chem. Res. 2022, 61, 4951–4970

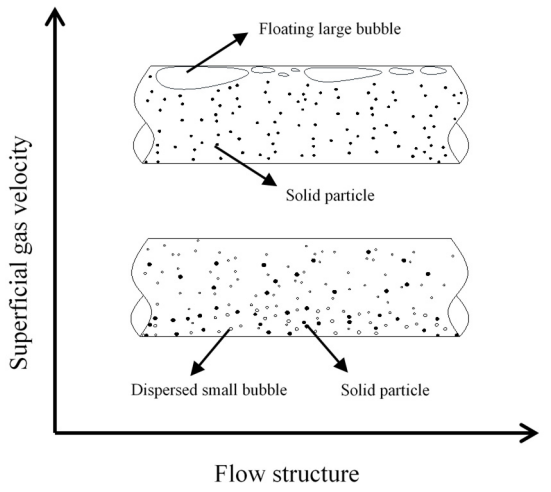

Figure 28. Schematic of mixed liquid flow structures at different gas velocities.

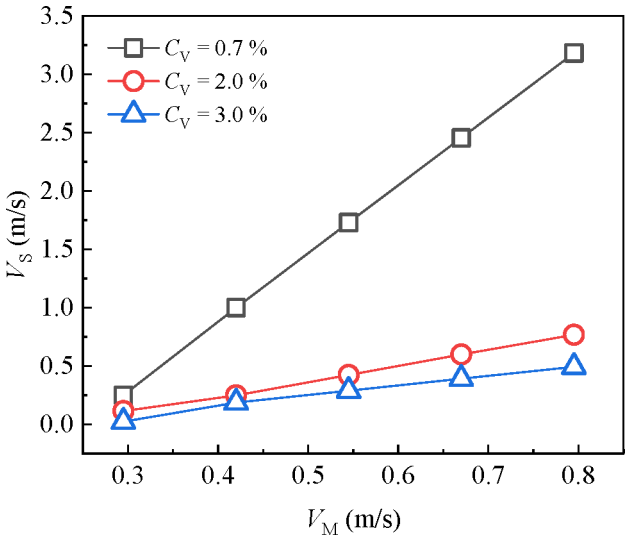

Figure 29. Relationship between the apparent wall slip velocity and the mixture velocity of gas/liquid−solid flow under different solid volume fractions

uniform, the gas velocity increases, and the Lockhart−Martenelli parameter value gradually decreases. The flow structure in the pipeline can thus be preliminarily determined by the change in the Lockhart−Martenelli parameter value.

4.3.2. Effect of Gas on the Apparent Wall Slip. According to Equation 5, the relationship between $(8\ V_{SL}/D)/\tau_w$ and $1/\varepsilon$ under the given shear stress is shown in Figure 25. It shows that the slope of the straight line is the corresponding $8C_D$ value, and the apparent wall slip coefficient C_D under the current working condition is obtained. The wall slip coefficient increases slightly with an increase in the superficial gas velocity under a small solid volume fraction; when the solid fraction is large, the influence of gas on the slip coefficient is negligible. This is because under the condition of a low solid content, the increase in the gas velocity is conducive to the formation and development of a uniform flow in the pipeline, and the effect of the increase in viscosity caused by the high solid content is much greater than that of gas. When the superficial gas velocity is a constant value, as the solid phase volume fraction increases, the overall curve in the figure shifts significantly, indicating that the ratio of the shear rate to

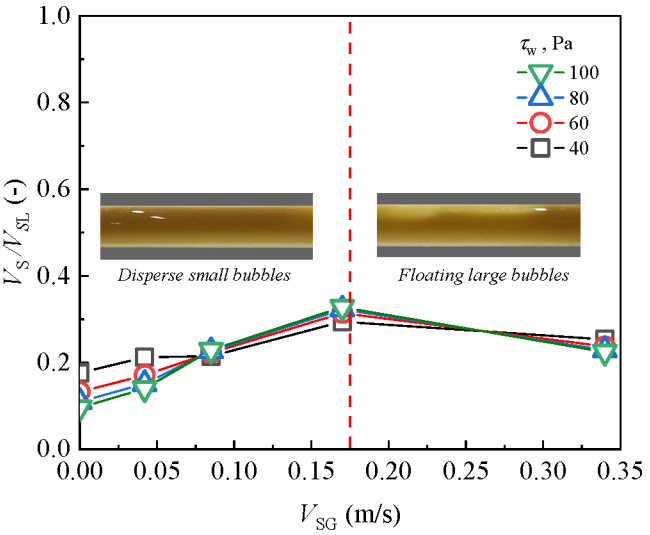

Figure 30. Relationship between the relative slip contribution and the gas volume fraction in gas/liquid−solid flow.

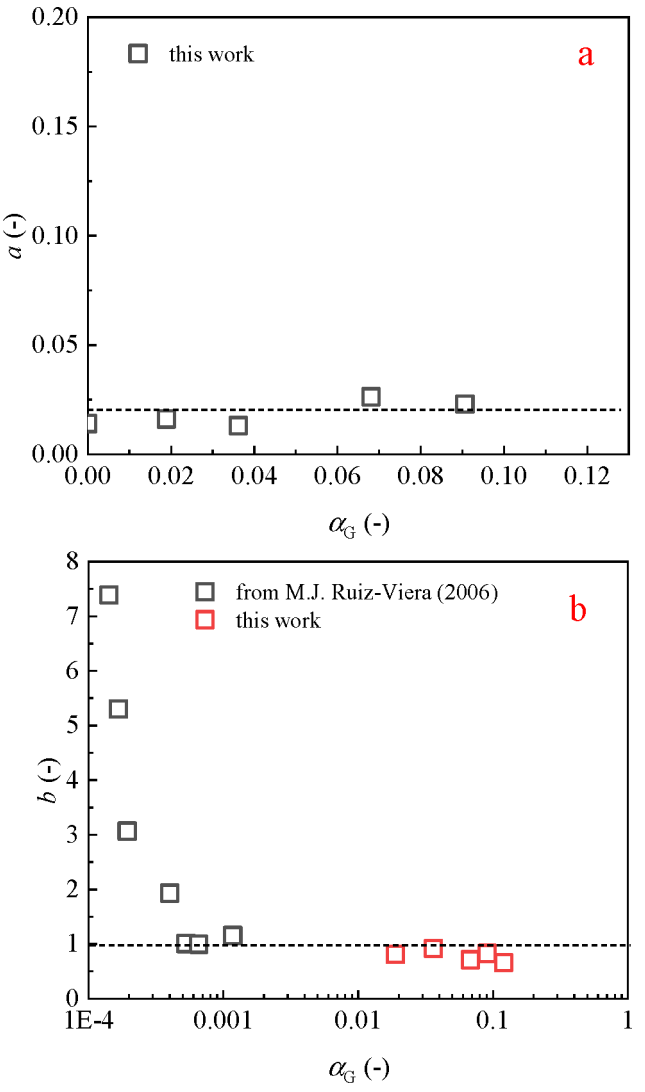

Figure 31. Variation in parameters a and b as a function of the gas volume fraction.

https://doi.org/10.1021/acs.iecr.1c04797
Ind. Eng. Chem. Res. 2022, 61, 4951−4970

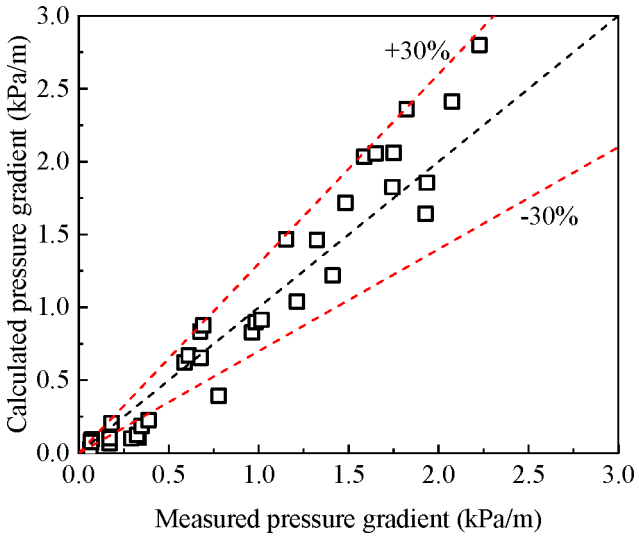

Figure 32. Comparison between the calculated and measured pressure gradient of the gas−liquid horizontal flow.

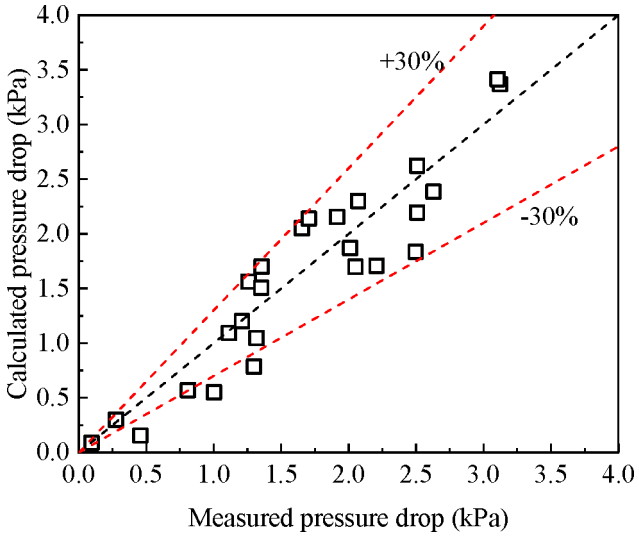

Figure 33. Comparison between the calculated and measured pressure gradient of the liquid−solid mixture in a horizontal pipe flow.

the wall shear force shows a decreasing trend; that is, the mixture viscosity of the fluid increases in the pipe.

Figure 26 shows the changing law of the sliding coefficient for different wall shear stresses. When the superficial gas velocity is constant, the sliding coefficient is positively related to the wall shear stress.

The pipe flow characteristics of the oil−sand mixture are similar to those of the oil and gas two-phase pipe flow, and the apparent wall slip velocity can also be expressed as a power law relationship with the wall shear stress. However, the participation of gas has a significant impact on the apparent wall−slip effect. Figure 27 shows the variation in the apparent wall slip velocity over a wide range of superficial gas velocities with different wall shear stresses. Under the condition of a fixed solid fraction, the apparent slip velocity first increases and then decreases with an increase in the superficial gas velocity. At the beginning, the gas velocity is at a low level, and the gas dispersed in the liquid promotes an increase in the mixture velocity, resulting in an increase in the slip velocity; when the gas phase

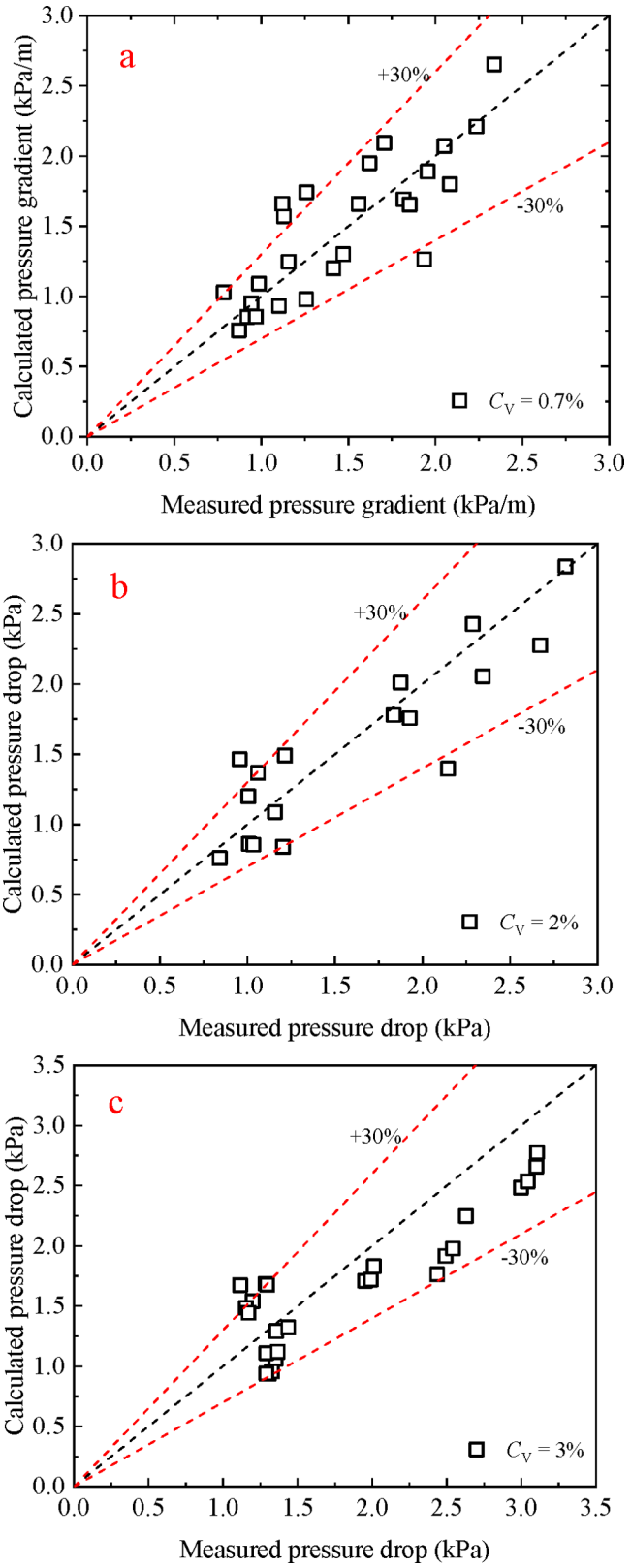

Figure 34. Comparison between the calculated and measured pressure gradients of the gas−liquid−solid mixture in a horizontal pipe flow: (a) C_V = 0.7%, (b) C_V = 2%, (c) C_V = 3%.

velocity increases to a higher level, bubbles coalesce. Under the action of gravity, large bubbles float onto the upper wall of the pipeline, and the gas occupies the wall area, which reduces the

https://doi.org/10.1021/acs.iecr.1c04797
Ind. Eng. Chem. Res. 2022, 61, 4951−4970

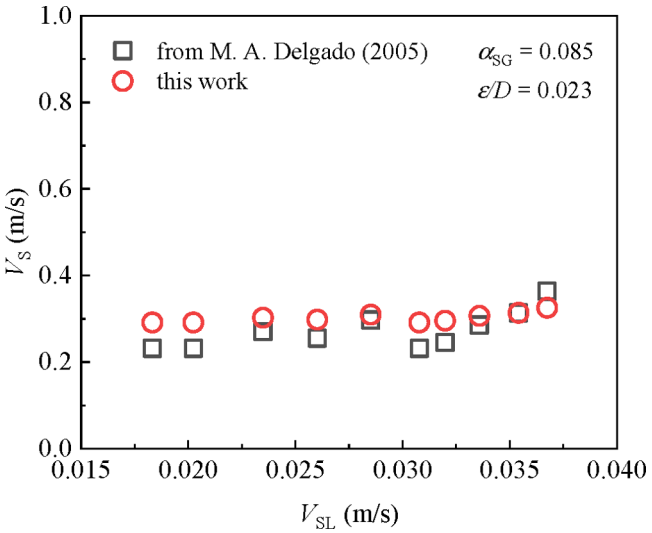

Figure 35. Comparison of the predictive model of this work with published the experimental data of Delgado et al.[33]

apparent slip velocity. This can be better understood in Figure 28.

In addition, in the gas−liquid−solid coupling flow system, the influence of the solid volume fraction cannot be ignored. As shown in Figure 29, with an increasing solid volume fraction, the apparent slip velocity decreases significantly. Notably, the wall slip phenomenon is more obvious at a lower solid fraction (C_V = 0.7%), which confirms that a small amount of solid particles in the mixture will fill the rough inner wall of the pipeline to form a lubricating layer, thus increasing the wall slip effect.

Figure 30 shows the variation in the relative slip contribution rate with superficial gas velocity when the gas/liquid−solid mixture flows in a PMMA pipe. As can be observed, the relative slip contribution first increases with an increase in the superficial gas velocity, but when the gas velocity exceeds 0.175 m/s, the relative slip contribution decreases. The main reason for this is that when the gas velocity is small, the increase in gas fraction promotes movement of the solid particles deposited at the bottom of the mixture along the pipe wall and increases the mixture velocity, which will cause an increase in the slip effect. However, in the fully developed pipe flow, the increase in gas

Table A-1. Experimental Data of Gas−Liquid Horizontal Pipe Flow

gas−liquid flow									
D (mm)	ε (mm)	V_{SG}(m/s)	V_{SL}(m/s)	$\Delta P/L$ (kPa)	D (mm)	ε (mm)	V_{SG}(m/s)	V_{SL}(m/s)	$\Delta P/L$ (kPa)
50.00	0.01	0.00	3.75	9.03	50.00	0.30	0.42	2.67	7.20
50.00	0.01	0.00	2.63	6.92	50.00	0.30	0.42	2.05	5.69
50.00	0.01	0.00	2.09	5.34	50.00	0.30	0.42	1.24	3.80
50.00	0.01	0.00	1.51	3.69	50.00	0.30	0.42	0.60	2.06
50.00	0.01	0.00	0.90	2.01	50.00	0.30	0.42	0.40	1.39
50.00	0.01	0.00	0.60	1.40	50.00	0.30	0.82	3.65	8.87
50.00	0.01	0.21	3.76	8.53	50.00	0.30	0.82	2.58	6.75
50.00	0.01	0.21	2.52	6.62	50.00	0.30	0.82	1.98	5.54
50.00	0.01	0.21	1.87	5.08	50.00	0.30	0.82	1.54	3.72
50.00	0.01	0.21	1.22	3.65	50.00	0.30	0.82	1.01	1.97
50.00	0.01	0.21	0.66	1.92	50.00	0.30	0.82	0.65	1.38
50.00	0.01	0.21	0.36	1.32	50.00	0.30	0.82	0.34	1.21
50.00	0.01	0.42	3.61	8.71	50.00	1.00	0.00	3.75	10.61
50.00	0.01	0.42	2.67	6.77	50.00	1.00	0.00	2.63	7.64
50.00	0.01	0.42	2.05	5.08	50.00	1.00	0.00	2.09	6.06
50.00	0.01	0.42	1.24	3.66	50.00	1.00	0.00	1.51	4.12
50.00	0.01	0.42	0.60	1.90	50.00	1.00	0.00	0.90	2.24
50.00	0.01	0.42	0.40	1.32	50.00	1.00	0.00	0.60	1.50
50.00	0.01	0.82	3.65	8.09	50.00	1.00	0.21	3.76	10.02
50.00	0.01	0.82	2.58	6.45	50.00	1.00	0.21	2.52	7.31
50.00	0.01	0.82	1.98	4.82	50.00	1.00	0.21	1.87	5.76
50.00	0.01	0.82	1.54	3.57	50.00	1.00	0.21	1.22	4.08
50.00	0.01	0.82	1.01	1.89	50.00	1.00	0.21	0.66	2.14
50.00	0.01	0.82	0.65	1.23	50.00	1.00	0.21	0.36	1.41
50.00	0.01	0.82	0.34	1.04	50.00	1.00	0.42	3.61	9.86
50.00	0.30	0.00	3.75	9.41	50.00	1.00	0.42	2.67	7.56
50.00	0.30	0.00	2.63	7.42	50.00	1.00	0.42	2.05	5.82
50.00	0.30	0.00	2.09	5.70	50.00	1.00	0.42	1.24	3.96
50.00	0.30	0.00	1.51	3.81	50.00	1.00	0.42	0.60	2.11
50.00	0.30	0.00	0.90	2.08	50.00	1.00	0.42	0.40	1.41
50.00	0.30	0.00	0.60	1.45	50.00	1.00	0.82	3.65	9.75
50.00	0.30	0.21	3.76	8.89	50.00	1.00	0.82	2.58	7.45
50.00	0.30	0.21	2.52	7.10	50.00	1.00	0.82	1.98	5.76
50.00	0.30	0.21	1.87	5.42	50.00	1.00	0.82	1.54	3.89
50.00	0.30	0.21	1.22	3.76	50.00	1.00	0.82	1.01	2.06
50.00	0.30	0.21	0.66	1.99	50.00	1.00	0.82	0.65	1.39
50.00	0.30	0.21	0.36	1.37	50.00	1.00	0.82	0.34	1.17

https://doi.org/10.1021/acs.iecr.1c04797
Ind. Eng. Chem. Res. 2022, 61, 4951−4970

Table A-2. Experimental Data of Liquid−Solid Horizontal Pipe Flow

liquid−solid flow				
D (mm)	ε (mm)	C_V (%)	V_{SL}(m/s)	$\Delta P/L$ (kPa)
50.00	0.01	0.00	2.23	2.50
50.00	0.01	0.00	1.89	2.21
50.00	0.01	0.00	1.55	1.92
50.00	0.01	0.00	1.38	1.65
50.00	0.01	0.00	1.12	1.32
50.00	0.01	0.00	0.90	1.00
50.00	0.01	0.00	0.70	0.81
50.00	0.01	0.00	0.45	0.46
50.00	0.01	0.00	0.21	0.28
50.00	0.01	0.00	0.08	0.09
50.00	0.01	0.70	1.98	2.51
50.00	0.01	0.70	1.63	2.05
50.00	0.01	0.70	1.28	1.71
50.00	0.01	0.70	0.94	1.26
50.00	0.01	0.70	0.63	1.13
50.00	0.01	0.70	0.42	1.12
50.00	0.01	0.70	0.20	1.13
50.00	0.01	2.00	1.82	3.12
50.00	0.01	2.00	1.46	2.51
50.00	0.01	2.00	1.16	2.07
50.00	0.01	2.00	0.86	1.30
50.00	0.01	2.00	0.58	1.11
50.00	0.01	2.00	0.39	1.21
50.00	0.01	2.00	0.19	1.08
50.00	0.01	3.00	1.84	3.10
50.00	0.01	3.00	1.46	2.63
50.00	0.01	3.00	1.19	2.01
50.00	0.01	3.00	0.94	1.35
50.00	0.01	3.00	0.62	1.36
50.00	0.01	3.00	0.44	1.44
50.00	0.01	3.00	0.22	1.20

fraction leads to a decrease in the contact area between the mixture and the pipe wall. Therefore, the relative slip contribution decreases with an increasing gas fraction.

4.4. Simplified Model of Apparent Wall Slip. *4.4.1. Apparent Wall Slip Effects in Gas/Liquid Two-Phase Pipe Flow.* Some researchers have studied the relationship between the slip velocity and wall shear stress of a suspension and gas lubricant two-phase flow in pipelines and found that the relationship between the slip velocity and wall shear stress can be expressed by a power law function:[48−50]

$$V_S = a\tau_w^{\ b} \tag{22}$$

where a and b are the coefficient and power-law exponent in the power-law function relationship, respectively. By connecting Equations 6 and 22, we obtain Equation 23. It should be noted that parameters a and b are obtained from a linear regression ($R^2 > 0.99$).

$$a = \frac{C_D\tau_w^{\ 1-b}}{\varepsilon / D} \tag{23}$$

The results in Figure 31a show that parameter a does not change with the gas phase volume fraction, but essentially fluctuates around a constant value of 0.02. The relationship between parameter b and the gas volume fraction is a power function. In the experimental study of M. J. Ruiz-Viera et al.,[34] when the gas volume fraction is low, with an increase in the gas fraction, parameter b first decreases and then tends to be constant at 1. The experimental study of this work was performed under the condition that the gas fraction is greater than 1%. Within the range of the gas fraction, parameter b essentially fluctuates around a constant value of 1, which is consistent with previous research results. Therefore, this work further puts forward a slip velocity model, which will expand the research scope. Parameter b and the gas volume fraction meet the following requirements:

$$b = 1.33 \times 10^{-5}\alpha_G^{\ -1.48} + 0.99 \tag{24}$$

Here, the range of the gas fraction ranges from 0% to 20%, excluding the case in which the gas volume fraction is 0. By introducing the expression of parameter b into Equation 18, the prediction model of the wall slip of gas−liquid two-phase horizontal flow can be obtained as follows

$$V_S = 0.02\tau_w^{\ (1.33\times10^{-5}\alpha_G^{\ -1.48}+0.99)} \tag{25}$$

The pressure gradient is calculated by using the above-mentioned apparent slip velocity model of gas−liquid pipeline flow and the calculated value is compared with the measured value (as shown in Figure 32). The results show that the error is essentially within 30%, which shows that the slip velocity model has an acceptable prediction effect.

4.4.2. Apparent Wall Slip Effects in Liquid/Solid Mixture Pipe Flow. The characteristics of liquid−solid mixed flow show that the apparent slip velocity is a power function of the wall shear stress. Through an analysis of the experimental data, the dimensionless parameter J related to the solid volume fraction is introduced:

$$J = \frac{\rho_{SL}}{\rho_{SL}(1 - C_V) + \rho_S C_V} \tag{26}$$

The dimensionless parameter J introduces the density and volume fraction of solid particles and represents the weight of the phase medium by the ratio of the liquid density to the liquid−solid mixture density. By analyzing experimental data, the apparent wall slip velocity model of liquid−solid mixed flow in a horizontal pipe is obtained:

$$V_S = 0.00189C_V^{\ -0.63}\tau_w^{\ 0.58}\frac{\rho_{SL}}{\rho_{SL}(1 - C_V) + \rho_S C_V} \tag{27}$$

The pressure gradient is calculated by using the apparent slip velocity model of the liquid−solid mixed flow. The calculated value of the pressure gradient was compared with the measured value. Figure 33 shows that the error is essentially controlled within 30%, which indicates that the slip velocity model has an acceptable prediction effect.

4.4.3. Apparent Wall Slip Effects in Gas/Liquid−Solid Mixed Pipe Flow. The apparent wall slip characteristics of gas/liquid−solid mixtures in a horizontal pipe flow are similar to those of a gas−liquid two-phase flow, assuming that the wall shear stress and slip velocity of the gas/liquid−solid flow show a power-law relationship, such as in Equations 22 and 23.

The wall slip characteristics of gas/liquid−solid mixed flows in horizontal pipes are closely related to the laws of gas−liquid two-phase and liquid−solid mixed flows. In this work, considering the characteristics of the slip velocity of gas−liquid and liquid−solid flows, it is assumed that the basic form of the wall slip velocity model of the gas−liquid−solid mixed flow is as follows

https://doi.org/10.1021/acs.iecr.1c04797
Ind. Eng. Chem. Res. 2022, 61, 4951−4970

Table A-3. Experimental Data of Gas/Liquid−Solid Horizontal Pipe Flow

gas/liquid−solid flow											
D (mm)	ε (mm)	C_V (%)	V_{SG}(m/s)	V_{SL}(m/s)	$\Delta P/L$ (kPa)	D (mm)	ε (mm)	C_V (%)	V_{SG}(m/s)	V_{SL}(m/s)	$\Delta P/L$ (kPa)
50.00	0.01	0.70	0.00	1.98	2.51	50.00	0.30	0.70	0.09	0.93	1.24
50.00	0.01	0.70	0.00	1.63	2.05	50.00	0.30	0.70	0.09	0.62	1.12
50.00	0.01	0.70	0.00	1.28	1.71	50.00	0.30	0.70	0.09	0.42	1.17
50.00	0.01	0.70	0.00	0.94	1.26	50.00	0.30	0.70	0.09	0.20	1.08
50.00	0.01	0.70	0.00	0.63	1.13	50.00	0.30	0.70	0.34	1.89	2.45
50.00	0.01	0.70	0.00	0.42	1.12	50.00	0.30	0.70	0.34	1.55	2.13
50.00	0.01	0.70	0.00	0.20	1.13	50.00	0.30	0.70	0.34	1.21	1.60
50.00	0.01	0.70	0.09	1.94	2.24	50.00	0.30	0.70	0.34	0.89	1.12
50.00	0.01	0.70	0.09	1.60	1.85	50.00	0.30	0.70	0.34	0.60	1.06
50.00	0.01	0.70	0.09	1.25	1.47	50.00	0.30	0.70	0.34	0.40	1.03
50.00	0.01	0.70	0.09	0.93	1.10	50.00	0.30	0.70	0.34	0.19	0.95
50.00	0.01	0.70	0.09	0.62	1.07	50.00	1.00	0.70	0.00	1.98	3.19
50.00	0.01	0.70	0.09	0.42	1.11	50.00	1.00	0.70	0.00	1.63	2.70
50.00	0.01	0.70	0.09	0.20	1.06	50.00	1.00	0.70	0.00	1.28	2.13
50.00	0.01	0.70	0.34	1.89	1.94	50.00	1.00	0.70	0.00	0.94	1.49
50.00	0.01	0.70	0.34	1.55	1.62	50.00	1.00	0.70	0.00	0.63	1.31
50.00	0.01	0.70	0.34	1.21	1.26	50.00	1.00	0.70	0.00	0.42	1.38
50.00	0.01	0.70	0.34	0.89	0.92	50.00	1.00	0.70	0.00	0.20	1.24
50.00	0.01	0.70	0.34	0.60	0.87	50.00	1.00	0.70	0.09	1.94	2.94
50.00	0.01	0.70	0.34	0.40	0.92	50.00	1.00	0.70	0.09	1.60	2.35
50.00	0.01	0.70	0.34	0.19	0.78	50.00	1.00	0.70	0.09	1.25	1.94
50.00	0.30	0.70	0.00	1.98	2.95	50.00	1.00	0.70	0.09	0.93	1.33
50.00	0.30	0.70	0.00	1.63	2.48	50.00	1.00	0.70	0.09	0.62	1.16
50.00	0.30	0.70	0.00	1.28	1.93	50.00	1.00	0.70	0.09	0.42	1.13
50.00	0.30	0.70	0.00	0.94	1.34	50.00	1.00	0.70	0.09	0.20	1.09
50.00	0.30	0.70	0.00	0.63	1.27	50.00	1.00	0.70	0.34	1.89	2.72
50.00	0.30	0.70	0.00	0.42	1.32	50.00	1.00	0.70	0.34	1.55	2.21
50.00	0.30	0.70	0.00	0.20	1.17	50.00	1.00	0.70	0.34	1.21	1.82
50.00	0.30	0.70	0.09	1.94	2.72	50.00	1.00	0.70	0.34	0.89	1.14
50.00	0.30	0.70	0.09	1.60	2.28	50.00	1.00	0.70	0.34	0.60	1.10
50.00	0.30	0.70	0.09	1.25	1.73	50.00	1.00	0.70	0.34	0.40	1.39

$$V_S = m(V_S)_{GL}{}^n J^q \tag{28}$$

where V_S represents the apparent wall slip velocity of the gas−liquid−solid three-phase flow in the pipeline, $(V_S)_{GL}$ is the wall slip velocity model of the gas−liquid pipe flow, and J is a dimensionless parameter related to solid particles.

Theoretical research (Mooney 1931;[43] Yilmazer and Kalyon 1989[48]) and experimental studies in this work have confirmed that the wall slip velocity (V_S) is power-law dependent on the wall shear stress (τ_w). In addition, the analysis results in this work show that the exponent (b) of the shear stress has a power-law relationship with the gas volume fraction (α). On the basis of the above theories, a prediction model of the wall slip velocity of gas−liquid two-phase flow is proposed, which is suitable for a wide gas fraction range. In addition, the volume fraction of solid particles (C_V) and the related dimensionless parameter (J) are introduced. The experimental data show that the dimensionless parameter term and wall shear stress term have a linear relationship with the wall slip velocity in the double logarithmic coordinate system, which meets the linear superposition principle.

By regression analyzing the experimental data of the gas−liquid−solid flow, the parameters in the calculation formula of slip velocity are determined, and the apparent slip velocity model is as follows

$$V_S = 0.00126 C_V{}^{-1.35}(0.02\tau_w{}^{1.33\times10^{-5}\alpha_G{}^{-1.48}+0.99})^{1.78}\left(\frac{\rho_{SL}}{\rho_{SL}(1-C_V)+\rho_S C_V}\right)^{-10.12} \tag{29}$$

The slip velocity model is used to calculate the predicted pressure gradient and compare it with the pressure gradient measured in the experiment. Figure 34 shows the consistency between the measured pressure gradient and the calculated pressure gradient at three solid volume fractions. The results show that the prediction effect of the proposed model is acceptable.

In general, the prediction model of the apparent wall slip velocity of gas−liquid−solid coupled flow in horizontal pipes has a good applicability when the gas fraction is 0−20% and the solid volume fraction is 0−3%. In addition, with the help of published experimental data, the better prediction effect of this model is further verified (as shown in Figure 35).

5. CONCLUSION

In this work, the behavior characteristics and influencing factors of a gas−liquid−solid mixed flow in horizontal pipes were studied. On the basis of experimental data and theoretical analysis, a calculation model of the wall slip velocity of gas−liquid−solid coupled flow in a horizontal pipe was proposed. The results of this work will be helpful for deeply understanding the characteristics of multiphase flow and the wall slip effect.

https://doi.org/10.1021/acs.iecr.1c04797
Ind. Eng. Chem. Res. 2022, 61, 4951−4970

The research results of gas−liquid and liquid−solid two-phase flow show that the pipe roughness and pipe size have different effects on the flow pressure gradient. It should be noted that the different liquid velocities will change the mixed flow structure of solid particles in the horizontal pipe. There is a critical liquid velocity to determine whether solid particles are deposited in the pipe, which is between 0.75 and 1 m/s. By defining the dimensionless parameters related to solid particles, the function of solid particles in the flow is further discussed. In addition, it is determined that, on the one hand, in the gas/liquid−solid mixture flow system the existence of gas will occupy the wall space and reduce the wall slip effect. On the other hand, gas can reduce the resistance and increase the wall slip effect. According to the experimental and theoretical analysis, it is proposed that the critical gas velocity is approximately 0.175 m/s.

On the basis of the wall slip theory of a single-phase flow and the experimental data of a multiphase flow in a horizontal pipe, a power-law model of the wall slip velocity for gas−liquid−solid mixed flow was proposed. Validation of experimental data showed that the prediction error of the model is acceptable. In general, although this model has some limitations, it has a certain significance for understanding the mechanism and influencing factors of the wall slip effect in multiphase flow systems.

APPENDIX: TEST DATA

Tables A-1, A-2, and A-3 contain test data from this work.

AUTHOR INFORMATION

Corresponding Author

Jingyu Xu − *Institute of Mechanics, Chinese Academy of Sciences, Beijing 100190, China; School of Engineering Sciences, University of Chinese Academy of Sciences, Beijing 100049, China;* orcid.org/0000-0002-1058-2257; Email: xujingyu@imech.ac.cn

Authors

Lintong Hou − *Institute of Mechanics, Chinese Academy of Sciences, Beijing 100190, China; School of Engineering Sciences, University of Chinese Academy of Sciences, Beijing 100049, China*

Dong Zhang − *Institute of Mechanics, Chinese Academy of Sciences, Beijing 100190, China*

Meng Yang − *Institute of Mechanics, Chinese Academy of Sciences, Beijing 100190, China; School of Engineering Sciences, University of Chinese Academy of Sciences, Beijing 100049, China*

Shuo Liu − *Institute of Mechanics, Chinese Academy of Sciences, Beijing 100190, China*

Complete contact information is available at: https://pubs.acs.org/10.1021/acs.iecr.1c04797

Notes

The authors declare no competing financial interest.

ACKNOWLEDGMENTS

The authors gratefully acknowledge that the work described here is financially supported by National Natural Science Foundation of China (No. 51779243) and the Strategic Priority Research Program of the Chinese Academy of Science (Grant No. XDB22030101).

NOMENCLATURE

C_V = solid volume holdup
C_D = slip coefficient
D = pipe internal diameter, m
$\Delta P/L$ = pressure gradient, kPa/m
Q = flow rate, m^3/h
R = pipe internal radius, m
Re_L = liquid Reynolds number
Re_M = mixture Reynolds number
V = mean velocity, m/s
V_{SL} = superficial liquid velocity, m/s
V_{SG} = superficial gas velocity, m/s
V_M = mixture velocity, m/s
V_S = apparent wall slip velocity, m/s
V_S/V_{SL} = relative slip contribution

Greek letters

α_G = gas volume fraction
$\dot{\gamma}$ = shear rate, s^{-1}
E = absolute pipe roughness, mm
ε/D = relative pipe roughness
M = apparent viscosity, mPa·s
μ_{LM} = apparent viscosity of liquid−solid mixture, mPa·s
ρ_L = liquid density, kg/m^3
ρ_{LM} = the density of liquid−solid mixture, kg/m^3
ρ_M = mixture density, kg/m^3
T = shear stress, Pa
τ_w = wall shear stress, Pa
Φ_L^2 = Lockhart−Martenelli parameter

REFERENCES

(1) Chavan, P. V.; Thombare, M. A.; Bankar, S. B.; Kalaga, D. V.; Patil-Shinde, V. A. Novel multistage solid−liquid circulating fluidized bed: Hydrodynamic characteristics. *Particuology.* **2018**, *38*, 134−142.

(2) Gu, J.; Fan, F.; Li, Y.; Yang, H.; Su, M.; Cai, X. Modeling and prediction of ultrasonic attenuations in liquid−solid dispersions containing mixed particles with Monte Carlo method. *Particuology.* **2019**, *43*, 84−91.

(3) Taitel, Y.; Dukler, A. E. A model for predicting flow regime transitions in horizontal and near horizontal gas-liquid flow. *AIChE J.* **1976**, *22*, 47−55.

(4) Xu, J. Y.; Wu, Y. X.; Li, H.; Guo, J.; Chang, Y. Study of drag reduction by gas injection for power-law fluid flow in horizontal stratified and slug flow regimes. *Chem. Eng. J.* **2009**, *147*, 235−244.

(5) Picchi, D.; Poesio, P. Stability of multiple solutions in inclined gas/shear-thinning fluid stratified pipe flow. *Int. J. Multiphase Flow.* **2016**, *84*, 176−187.

(6) Hou, L. T.; Liu, S.; Zhang, J.; Xu, J. Y. Evaluation of the behavioral characteristics in a gas and heavy oil stratified flow according to the Herschel-Bulkley fluid model. *ACS Omega.* **2020**, *5*, 17787−17800.

(7) Medhi, B. J.; Kumar, A. A.; Singh, A. Apparent wall slip velocity measurements in free surface flow of concentrated suspensions. *International Journal of Multiphase Flow* **2011**, *37* (6), 609−619.

(8) Hanks, R. W.; Hanks, K. W.A new viscometer for determining the effect of particle size distributions and concentration on slurry rheology. *Proceedings of 7th International Technical Conference on Slurry Transportation*, Lake Tahoe, NV, 1982.

(9) Ma, X. Y.; Duan, Y. F.; Li, H. F. Wall slip and rheological behavior of petroleum-coke sludge slurries flowing in pipelines. *Powder Technol.* **2012**, *230*, 127−133.

(10) Worrall, W. E.; Tuliani, S. Viscosity changes during the ageing of clay-water suspensions. *Trans. Br. Ceram. Soc.* **1964**, *63*, 167−185.

(11) Xu, J. Y.; Huhe, A. Rheological study of mudflows at lianyungang in China. *Int. J. Sediment Res.* **2016**, *31*, 71−78.

(12) Huang, Z.; Aode, H. A laboratory study of rheological properties of mudflows in Hangzhou Bay. *China, Int. J. Sediment Res.* **2009**, *24* (4), 410−424.
(13) Senapati, P. K.; Mishra, B. K.; Parida, A. Modeling of viscosity for power plant ash slurry at higher concentrations: Effect of solids volume fraction, particle size and hydrodynamic interactions. *Powder Technol.* **2010**, *197* (1−2), 1−8.
(14) Konijn, B. J.; Sanderink, O. B. J.; Kruyt, N. P. Experimental study of the viscosity of suspensions: Effect of solid fraction. particle size and suspending liquid. *Powder Technol.* **2014**, *266* (6), 61−69.
(15) Gutierrez, L.; Pawlik, M. Observations on the yielding behaviour of oil sand slurries under vane and slump tests. *Can. J. Chem. Eng.* **2015**, *93* (8), 1392−1402.
(16) Zhang, J.; Zhao, H.; Li, W.; Xu, M. H.; Liu, H. F. Multiple effects of the second fluid on suspension viscosity. *Sci. Rep.* **2015**, *5*, 16058.
(17) Ren, T.; Mu, H.; Liu, S.; Sun, Y.; Zhang, J.; Liu, S. Prediction of gas-liquid two-phase heat transfer coefficient. *Appl. Therm. Eng.* **2017**, *116*, 217−232.
(18) Zhang, J.; Yuan, H.; Mei, N.; Yan, Z. Estimation of solid concentration in solid-liquid two-phase flow in horizontal pipeline using inverse problem approach. *Particuology.* **2022**, *62*, 1−13.
(19) Gillies, R. G.; Shook, C. A.; Wilson, K. C. An improved two layer model for horizontal slurry pipeline flow. *Can. J. Chem. Eng.* **1991**, *69*, 173−178.
(20) Kaushal, D.; Tomita, Y. Solids concentration profiles and pressure drop in pipeline flow of multisized particulate slurries. *Int. J. Multiphase Flow 28* **2002**, *28*, 1697−1717.
(21) Tang, C.; Liu, M.; Li, Y. Experimental investigation of hydrodynamics of liquid-solid mini-fluidized beds. *Particuology.* **2016**, *27*, 102−109.
(22) Ravelet, F.; Bakir, F.; Khelladi, S.; Rey, R. Experimental study of hydraulic transport of large particles in horizontal pipes. *Exp. Therm. Fluid Sci.* **2013**, *45*, 187−197.
(23) Xu, J. Y.; Wu, Y. X.; Shi, Z. H.; Lao, L. Y.; Li, D. H. Studies on two-phase co-current air/non-Newtonian shear-thinning fluid flows in inclined smooth pipes. *Int. J. Multiphase Flow.* **2007**, *33* (9), 948−969.
(24) Ribeiro, J. X. F.; Liao, R.; Aliyu, A. M.; Liu, Z. Prediction of pressure gradient in two and three-phase flows in vertical pipes using an artificial neural network model. *Int. J. Eng. Technol.* **2019**, *9* (3), 155−170.
(25) Ribeiro, J. X. F.; Liao, R.; Aliyu, A. M.; Baba, Y. D.; Archibong-Eso, A.; Ehinmowo, A.; Liu, Z. L. An assessment of gas void fraction prediction models in highly viscous liquid and gas two-phase vertical flows. *J. Nat. Gas Sci. Eng.* **2020**, *76*, 103107.
(26) Aliyu, A. M.; Almabrok, A. A.; Baba, Y. D.; Lao, L.; Yeung, H.; Kim, K. C. Upward gas-liquid two-phase flow after a U-bend in a large-diameter serpentine pipe. *Int. J. Heat Mass Transfer* **2017**, *108*, 784−800.
(27) Archibong-Eso, A.; Baba, Y.; Aliyu, A.; Ribeiro, J.; Abam, F.; Yeung, H. Particle-Transport Mechanism in Liquid/Liquid/Solid Multiphase Pipeline Flow of High-Viscosity Oil/Water/Sand. *SPE Journal.* **2021**, *26* (05), 2977−2992.
(28) Scott, D. S.; Rao, P. K. Transport of solids by gas-liquid mixtures in horizontal pipes. *Can. J. Chem. Eng.* **1971**, *49*, 302−309.
(29) Holte, S.; Anglesen, S.; Kvernvold, O.; Raesder, J. H.Sand bed formation in horizontal and near horizontal gas-liquid-sand flow. *European Two-Phase Flow Group Meeting*, Trondheim, Norway, 1987; p 205.
(30) Oudeman, P.Sand transport and deposition in horizontal multiphase trunklines of subsea satellite developments. *Offshore Technology Conference*; Offshore Technology Conference, 1992; Vol. *8*, pp 0−4.
(31) Fajemidupe, O. T.; Aliyu, A. M.; Baba, Y. D.; Archibong-Eso, A.; Yeung, H. Sand minimum transport conditions ingas-solid-liquid three-phase stratified flow in a horizontal pipe at low particle concentrations. *Chem. Eng. Res. Des.* **2019**, *143*, 114−126.
(32) Leporini, M.; Marchetti, B.; Corvaro, F.; di Giovine, G.; Polonara, P.; Terenzi, A. Sand transport in multiphase flow mixtures in a horizontal pipeline: An experimental investigation. *Petroleum* **2019**, *5* (2), 161−170.
(33) Delgado, M. A.; Franco, J. M.; Partal, P.; Gallegos, C. Experimental study of grease flow in pipelines: wall slip and air entrainment effects. *Chem. Eng. Process.* **2005**, *44*, 805−817.
(34) Ruiz-Viera, M. J.; Delgado, M. A.; Franco, J. M.; Gallegos, C. Evaluation of wall slip effects in the lubricating grease/air two-phase flow along pipelines. *J. Non-Newton Fluid Mech.* **2006**, *139* (3), 190−196.
(35) Ruiz-Viera, M. J.; Delgado, M. A.; Franco, J. M.; Sanchez, M. C.; Gallegos, C. On the drag reduction for the two-phase horizontal pipe flow of highly viscous non-Newtonian liquid/air mixtures: case of lubricating grease. *Int. J. Multiphase Flow.* **2006**, *32*, 232−247.
(36) Czarny, R.; Paszkowski, M.; Knop, P. The wall effect in the flow of commercial lubricating greases. *J. Tribol.* **2016**, *138* (3), 031803.
(37) Balan, C.; Franco, J. M. Influence of the geometry on the transient and steady flow of lubricating greases. *Tribol. Trans.* **2001**, *44*, 53−58.
(38) Barnes, H. A. A review of the slip (wall depletion) of polymer solutions, emulsions and particle suspensions in viscometers: its cause, character and cure. *J. Non-Newtonian Fluid Mech.* **1995**, *56*, 221−241.
(39) Sanchez, M. C.; Valencia, C.; Franco, J. M.; Gallegos, C. Wall slip phenomena in oil-in-water emulsions: effect of some structural parameters. *J. Colloid Interface Sci.* **2001**, *241*, 226−232.
(40) Nickerson, C. S.; Kornfield, J. A. A novel 'cleat' geometry for suppressing wall slip. *J. Rheol.* **2005**, *49*, 865−874.
(41) Kalyon, D. M. Comments on the use of rheometers with rough surfaces or surfaces with protrusions. *J. Rheol.* **2005**, *49*, 1153−1155.
(42) Chisholm, D.; Laird, A. D. K. Two-phase flow in rough tubes. *Trans. ASME* **1958**, *80*, 276−286.
(43) Mooney, M. Explicit formulas for slip and fluidity. *J. Rheol.* **1931**, *2* (2), 210−222.
(44) Kang, J. H.; Zhang, X. Y.; Zhang, D.; Liu, Y. K. Pressure drops and mixture friction factor for gas-liquid two-phase transitional flows in a horizontal pipe at low gas flow rates. *Chem. Eng. Sci.* **2021**, *246*, 117011.
(45) Feng, K.; Zhang, H. C. Pressure drop and flow pattern of gas-non-Newtonian fluid two-phase flow in a square microchannel. *Chem. Eng. Res. Des.* **2021**, *173*, 158−169.
(46) Bevington, P. R.; Robinson, O. K.*Data Reduction and Error Analysis for the Physical Sciences*, 3rd ed.; McGraw-Hill Press: Boston, 2003; pp 39−40.
(47) Kalyon, D. M.; Yaras, P.; Aral, B.; Yilmazer, U. Rheological behavior of a concentrated suspension: A solid rocket fuel simulant. *J. Rheol.* **1993**, *37* (1), 35−53.
(48) Yilmazer, U.; Kalyon, D. M. Slip effects in capillary and parallel disk torsional flows of highly filled suspensions. *J. Rheol.* **1989**, *33* (8), 1197−1212.
(49) Cohen, Y.; Metzner, A. B. Apparent slip flow of polymer solutions. *J. Rheol.* **1985**, *29* (1), 67−102.
(50) Kokini, J. L.; Dervisoglu, M. Wall effects in the laminar pipe flow of four semi-solid foods. *J. Food Eng.* **1990**, *11* (1), 29−42.

https://doi.org/10.1021/acs.iecr.1c04797
Ind. Eng. Chem. Res. 2022, 61, 4951−4970